PL-TR-97-2133

A MAGNETOSPHERIC NEUTRAL SHEET-ORIENTED COORDINATE SYSTEM FOR MSM AND MSFM APPLICATIONS

R. V. Hilmer

Boston College
Institute for Scientific Research
140 Commonwealth Avenue
Chestnut Hill, MA 02167
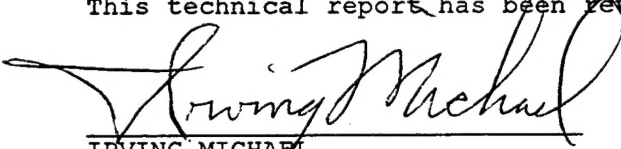
31 July 1997

Scientific Report No. 2

19980227 048

DTIC QUALITY INSPECTED 3

PHILLIPS LABORATORY
Directorate of Geophysics
AIR FORCE MATERIEL COMMAND
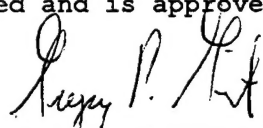**HANSCOM AIR FORCE BASE, MA 01731-3010**

This technical report has been reviewed and is approved for publication.

IRVING MICHAEL
Contract Manager
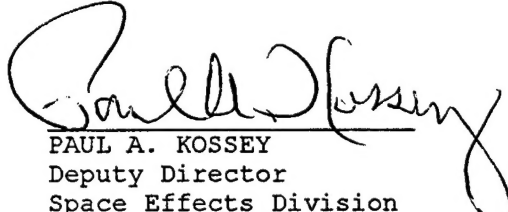Solar & Terrestrial Effects Branch
Space Effects Division

for MARK D. CONFER, Major, USAF
Chief
Solar & Terrestrial Effects Branch
Space Effects Division

PAUL A. KOSSEY
Deputy Director
Space Effects Division

This report has been reviewed by the ESC Public Affairs Office (PA) and is releasable to the National Technical Information Service (NTIS).

Qualified requestors may obtain additional copies from the Defense Technical Information Center. All others should apply to the National Technical Information Service.

If your address has changed, or if you wish to be removed from the mailing list, or if the addressee is no longer employed by your organization, please notify PL/TSI, Hanscom AFB, MA 01731-3010. This will assist us in maintaining a current mailing list.

Do not return copies of this report unless contractual obligations or notices on a specific document require that it be returned.

REPORT DOCUMENTATION PAGE

Public reporting burden for this collection of information is estimated to average 1 hour per response, including the time for reviewing instructions, searching existing data sources, gathering and maintaining the data needed, and completing and reviewing the collection of information. Send comments regarding this burden estimate or any other aspect of this collection of information, including suggestions for reducing this burden, to Washington Headquarters Services, Directorate for Information Operations and Reports, 1215 Jefferson Davis Highway, Suite 1204, Arlington, VA 22202-4302, and to the Office of Management and Budget, Paperwork Reduction Project (0704-0188), Washington, DC 20503.

1. AGENCY USE ONLY (Leave blank)	2. REPORT DATE 31 July 1997	3. REPORT TYPE AND DATES COVERED Scientific Report No. 2

4. TITLE AND SUBTITLE
A MAGNETOSPHERIC NEUTRAL SHEET—ORIENTED COORDINATE SYSTEM FOR MSM and MSFM APPLICATIONS

5. FUNDING NUMBERS
PE 63707F
PR 7601 TA GA
WU CB

Contract:
F19628-96-C-0030

6. AUTHOR(S)
R.V. Hilmer

7. PERFORMING ORGANIZATION NAME(S) AND ADDRESS(ES)
Boston College
Institute for Scientific Research
140 Commonwealth Avenue
Chestnut Hill, MA 02167-3862

8. PERFORMING ORGANIZATION REPORT NUMBER

9. SPONSORING/MONITORING AGENCY NAME(S) AND ADDRESS(ES)
Phillips Laboratory
29 Randolph Road
Hanscom AFB, MA 01731-3010
Contract Manager: Irving I. Michael/GPSG

10. SPONSORING/MONITORING AGENCY REPORT NUMBER
PL-TR-97-2133

11. SUPPLEMENTARY NOTES

12a. DISTRIBUTION/AVAILABILITY STATEMENT

Approved for public release; distribution unlimited

12b. DISTRIBUTION CODE

13. ABSTRACT (Maximum 200 words)

We develop an analytic magnetospheric neutral sheet-oriented coordinate system which depends on the Earth's dipole tilt angle, ψ, and the geomagnetic activity index Kp. With an orientation similar to that of the GSM coordinate system, this non-orthogonal coordinate system contains coordinate surfaces (at constant Z' values) which conform to a shape approximating that of the magnetic neutral sheet. By more accurately representing a point's location relative to the magnetic neutral sheet, use of this coordinate system should help improve the current procedure used to specify geomagnetic field values and derive three-dimensional energetic particle flux information from the two-dimensional simulation results provided by the Magnetospheric Specification Model (MSM) and Magnetospheric Specification and Forecast Model (MSFM). The procedure comprises the computer codes MAP3D and FLUX3D and is limited, as are the MSM and MSFM, by use of the approximation in the magnetic field configurations which fixes the dipole tilt angle equal to zero degrees. Under this condition, all magnetic field configurations are symmetric about the GSM equatorial plane which coincides with both the model simulation surface and the neutral sheet. When input is given in GSM coordinates, the MAP3D procedure pairs off-equatorial locations with inappropriate magnetic mapping points on the MSM/MSFM simulation surface owing to the actual ψ and Kp dependence of the magnetic neutral sheet position. It is suggested that improved magnetic field mappings, and thus improved specification of particle fluxes and magnetic field values, will result if all spatial points input to the MAP3D algorithm are expressed in terms of this new coordinate system rather than in GSM coordinates.

14. SUBJECT TERMS
magnetosphere, magnetic field, neutral sheet, magnetotail, dipole tilt angle, geomagnetic activity, coordinate systems, magnetospheric specification model, magnetic field mapping, energetic particle flux specification

15. NUMBER OF PAGES
54

16. PRICE CODE

17. SECURITY CLASSIFICATION OF REPORT	18. SECURITY CLASSIFICATION OF THIS PAGE	19. SECURITY CLASSIFICATION OF ABSTRACT	20. LIMITATION OF ABSTRACT
UNCLASSIFIED	UNCLASSIFIED	UNCLASSIFIED	SAR

Table of Contents

Figures:

1. Magnetic Field and Particle Flux Specification in the MSM/MSFM

1.1. Original Mapping Method

The *Hilmer and Voigt* [1995] magnetic field model provides the Magnetospheric Specification Model (MSM) [*Freeman et al.*, 1993] and Magnetospheric Specification and Forecast Model (MSFM) [*Bales et al.*, 1993] with equatorial magnetic field values, magnetic flux tube volumes, and a method for establishing one-to-one mappings between an ionospheric electric potential grid and a simulation grid contained within the GSM equatorial plane. Note that the MSM and MSFM utilize identical magnetic field treatments in all respects so all statements and conclusions herein apply equally to both. The MSM simulation grid is always aligned with the GSM equatorial plane owing to the zero dipole tilt approximation which was adopted to take advantage of North-South magnetic field symmetries and reduce the amount of pre-calculated magnetic field configuration information tabulated and stored off-line. Allowing the dipole tilt angle, ψ, to vary would introduce a fourth parameter space variable (the others being *Dst*, the magnetopause standoff distance, and the midnight equatorward auroral boundary) and would increase the number of magnetospheric configurations by at least a factor of five. The MSM algorithm utilizes stored magnetic field quantities because the on-line tracing of magnetic field lines is too computer intensive to be practical in an operational setting. These magnetic field quantities are used by the MSM to map the electric field (magnetic field lines are assumed to be equipotentials) to the equatorial plane and calculate adiabatic particle drift paths. By performing drift calculations on a variety of particle species over appropriate energy ranges, one of the MSM final outputs is the specification of particle fluxes in the magnetic equatorial plane.

A special procedure developed by *Hilmer et al.* [1993], commonly referred to by its FORTRAN subroutine name MAP3D, utilizes additional tabulated magnetic field information to obtain MSM particle flux and magnetic field information outside the GSM equatorial plane. In the MAP3D procedure, a 3-D grid was defined and magnetic field vector and equatorial mapping information stored for each grid point in each of 932 magnetospheric configurations spanning the 3-D parameter space. To represent actual geophysical conditions, the MAP3D algorithm interpolates magnetic field information from the eight closest configurations in the parameter space to form a unique configuration for each given time. Arbitrary points in space are then mapped to the MSM simulation region using this tailored field configuration and the corresponding equatorial fluxes are scaled (using the FLUX3D algorithm) to assign appropriate values to off-equatorial locations. As with the MSM particle drift algorithm mentioned above, this procedure takes advantage of the symmetry inherent in the magnetic field model when the tilt of the Earth's dipole field is fixed equal to zero degrees.

1.2. Mapping Problems

With the established procedure of providing location input in GSM coordinates regardless of the actual dipole tilt angle, the MAP3D algorithm has been used to extract reasonable particle flux values from the 2-D MSM simulation output under a variety of geophysical conditions and along very different orbits including the high inclination CRRES orbit. Recently, however, it was revealed that some unphysical magnetic field mappings were being produced by MAP3D with the implication that the MSM particle flux specifications would be adversely affected (*Prochaska*, Hughes STX Corporation - 23 April 1996 facsimile to Freeman of Rice University). *Prochaska* noticed on several different occasions that magnetic field lines from geosynchronous satellites on the nightside of the magnetosphere mapped to equatorial locations far tailward of geosynchronous altitudes, i.e., beyond $X_{GSM} = -20$ Re (Earth radii). This observation is most certainly indicative of a mapping problem as all dipole tilt-dependent magnetic field models we know of, including the *Hilmer and Voigt* [1995] model on which MAP3D is based, map geosynchronous orbit locations to neutral sheet locations within just a few Re of the satellite's position. Several causal factors were suggested including the presence of extremely stretched magnetic field lines in the midnight sector of the magnetotail and large satellite magnetic latitude deviations (> 11 degrees) as a function of geographic longitude. While both of these certainly contribute to magnetic field mappings beyond geosynchronous altitude, the overwhelming contributing factor involves the $\psi = 0$ approximation adopted within the MAP3D algorithm. Geosynchronous mapping examples illustrates this point.

First, we ran the MSM for a short period with $Kp = 3$ in order to use the MAP3D algorithm at $UT = 0500$ on day 354 of 1995 when the actual dipole tilt angle was $\psi = -34°$. The coordinates $(X_{GSM}, Y_{GSM}, Z_{GSM}) = (-6.065\,\text{Re}, -0.123\,\text{Re}, -2.626\,\text{Re})$ represent a point along the geosynchronous orbit at that time. With the $\psi = 0$ approximation, the eight magnetic field configurations interpolated by MAP3D scattered mappings from $X_{GSM} = -9$ to -37 Re such that the resultant mapping was located well down the magnetotail at $X_{GSM} = -27$ Re. Second, if this same mapping is done using the $Kp = 3$ version of the *Hilmer and Voigt* [1995] model with the dipole tilt angle also held at $\psi = 0$, this geosynchronous point maps to $X_{GSM} = -33$ Re. In both $\psi = 0$ cases, the starting point is located on moderately stretched tail-like field lines more than 2 Re below the magnetic neutral sheet (and the MSM simulation region). The neutral sheet is the surface defined by the local magnetic field strength minimum center in the plasma sheet and coincides with the GSM equatorial plane when $\psi = 0$. In fact, locations near the center of the magnetotail where $|Z_{GSM}| > 1.5$ to 2.0 Re and $X_{GSM} = -6.6$ Re often map well tailward of geosynchronous orbit when Kp is moderate to high and $\psi = 0$. Finally, if the actual value of $\psi = -34°$ is used in the *Hilmer and Voigt* [1995] model the magnetic neutral sheet is displaced below the GSM equatorial plane and our geosynchronous point maps more realistically to the

neutral sheet inside of $X_{GSM} = -7$ Re. This close mapping results directly from that fact that our point is closer to the neutral sheet which has, in this latter case, been properly displaced out of the GSM equatorial plane in response to a non-zero dipole tilt angle.

We conclude that the implementation of the MAP3D algorithm must be modified to incorporate the effects of dipole tilt angle variations on the magnetic field.

1.3. Proposed Solution

With $\psi = 0$, the GSM equatorial plane is coplanar with the MSM simulation region, extending approximately 10 Re sunward and 20 Re tailward of the Earth, and acts as a symmetry plane for the MAP3D field mapping algorithm. This approximation causes the plasma sheet and its imbedded magnetic neutral sheet to be artificially aligned with the GSM equatorial plane. To be more physical, the flat MSM simulation region should flex and follow the motion of the plasma and the magnetic neutral sheets as they are displaced from the GSM equatorial plane in response to phenomena such as dipole tilt angle changes, solar wind pressure variations, and the growth and decay of the ring and cross-tail currents. Accordingly, the MAP3D algorithm should incorporate the corresponding magnetic field configuration changes. As both of these alteration would require much additional research, testing, and computer storage with no guarantee of improving MSM particle flux specifications significantly, we propose a relatively simple solution in the form of a coordinate transformation that will allow the MSM and MAP3D algorithms to remain unchanged.

As mentioned above, while moving away from the neutral sheet of the magnetotail along the Z_{GSM} direction we cross field lines that map increasing farther tailward. Even within the MSM and MAP3D $\psi = 0$ framework, this fact means that we are encountering particles with gradually more distant neutral sheet crossing points and the particle fluxes extracted from MSM simulations using MAP3D are related to the flux levels at those same points. We are currently using the GSM coordinates of satellites to derive MSM flux levels using MAP3D regardless of the actual neutral sheet geometry. We need to modify the input position information provided to MAP3D to account for realistic motions of the neutral sheet.

To improve the magnetic field mappings used to derive particle flux specifications from both MSM and MSFM simulations, we propose providing the MAP3D algorithm with input coordinates based on a new magnetospheric neutral sheet-oriented coordinate system dependent on both the dipole tilt angle, ψ, and geomagnetic activity, Kp.

3

2. A Neutral Sheet-Oriented Coordinate System

### 2.1. Characteristics of the Neutral Sheet

For the purposes of this work, we identify the magnetospheric neutral sheet simply as the minimum magnetic field $|\mathbf{B}|$ surface found at low latitudes about the Earth at all local times. When the dipole tilt angle ψ is zero the magnetic field configuration becomes symmetric about the $Z_{GSM} = 0$ plane and the neutral sheet is coincident with the GSM equatorial plane. When $\psi \neq 0$, this alignment does not occur. For positive (negative) ψ, the neutral sheet is shifted above (below) the GSM equatorial plane at midnight as represented in Figure 1 (with $\psi = \psi'$). The neutral sheet bends gradually away from the SM equator to become aligned with the X_{GSM} axis at $Z_{GSM} = HD \sin \psi$, where HD is known as the "hinging" distance, and there is no tendency for it to return to the GSM equatorial plane at large distances [*Fairfield*, 1980]. As we move toward the flanks of the mid and far magnetotail the neutral sheet approaches the GSM equatorial plane and crosses it [e.g., *Fairfield*, 1980; *Dandouras*, 1988]. Away from local midnight, the near-Earth neutral sheet's deflection from the SM equatorial plane lessens as it joins the SM equatorial plan at dawn and dusk [*Lopez*, 1990]. Finally, on the dayside we assume for simplicity that the neutral sheet remains fixed in the SM equatorial plane which contains the local $|\mathbf{B}|$ minimum of the dipole field. As these various neutral sheet regions must connect smoothly to form a single surface, the neutral sheet must be continuously flexing and warping in response to the diurnal dipole tilt angle oscillations. Additionally, there is a tendency for the nightside neutral sheet to be displaced more from the GSM equatorial plane as geomagnetic activity decreases for a given value of ψ (see details in Section 2.3), a feature that is as least partially attributable to the existence of weaker cross-tail currents during these times. Without detailed quantitative information about how to model the neutral sheet's response to other more specific physical phenomena, e.g., solar wind pressure changes, we will concentrate on including an activity dependence via the geomagnetic index Kp in hopes that it will aide us in specifying neutral sheet behavior.

In the following, we derive a single analytic coordinate system (X', Y', Z') dependent on ψ and Kp such that the $Z' = 0$ surface coincides approximately with the neutral sheet. The GSM coordinates of satellite locations used previously to determine flux specification should be translated into this new coordinate system before being supplied to the MAP3D algorithm.

2.2. Dependence on Dipole Tilt Angle

The Coordinates X' and Z': The geometry used to organize the new coordinate system in a given GSM *X-Z* plane is shown in Figure 1. The SM coordinate system differs from GSM by a rotation equal to the dipole tilt angle ψ about the common $Y_{GSM} = Y_{SM}$ axis, namely

Neutral Sheet-Oriented Coordinate System
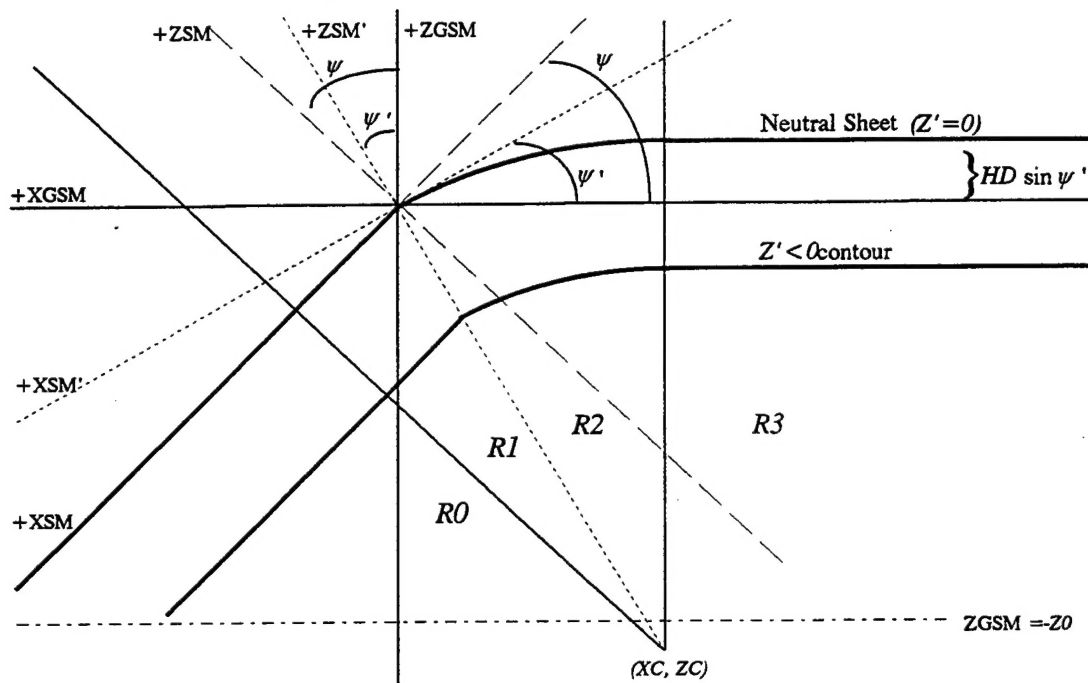
Schematic of neutral sheet-oriented coordinate system regions and boundaries in a GSM X-Z plane (Sun to the left). Contours of constant Z' are equidistant from the neutral sheet (at $Z' = 0$) while X' increases along them to the left and Y increases out of the page. The dipole tilt angle is ψ and the neutral sheet "hinging" distance, HD, varies with Kp. The angle ψ', equal to ψ at $Y_{GSM} = 0$, decreases in magnitude toward the flanks and $|\psi'| \le |\psi|$. The point (XC, ZC) acts as the center of curvature for the curved coordinate space in Region $R2$. Restrictive conditions include $|\psi| < 40$ degrees and $|Z_{GSM}| < Z0 = 17$ Re.

FIGURE 1

5

$$X_{SM} = X_{GSM} \cos \psi - Z_{GSM} \sin \psi$$

$$Y_{SM} = Y_{GSM} \tag{1}$$

$$Z_{SM} = X_{GSM} \sin \psi + Z_{GSM} \cos \psi$$

We define the new SM' coordinate system similarly except that its rotation angle ψ' varies with Y_{GSM}. A modified version of Eq. (10a) of *Dandouras* [1988], which incorporates a nominal "hinging" distance of 10.5 Re, is used to get the position of the neutral sheet, $Z_{GSM,NS}$, across the magnetotail for $X_{GSM} < XC$ and illustrates the relationship between the angle ψ' and Y_{GSM}, namely

$$Z_{GSM,NS} = \frac{HD}{10.5}\left[17\left(1 - \frac{Y_{GSM}}{225}\right)^{1/2} - 6.5\right]\sin \psi = HD \sin \psi' \quad \text{for } |Y_{GSM}| < 13.86\,\text{Re} \tag{2}$$

$$Z_{GSM,NS} = 0 \qquad\qquad\qquad\qquad\qquad \text{for} \quad |Y_{GSM}| \geq 13.86\,\text{Re}$$

The angle ψ' is largest and equal to ψ at the center of the magnetotail and decreases toward the flanks to $\psi' = 0$ for $|Y_{GSM}| \geq 13.86$ Re. The $Z' = 0$ contour is the line labeled as the neutral sheet while a sample negative Z' contour is indicated by the line running parallel to it. For $|Z_{GSM}| < Z0$, each plane is divided into Regions *R0, R1, R2,* and *R3*, separated by the three lines emanating from the center of curvature point (*XC, ZC*). The constant Z0 is selected to be just earthward of the smallest |ZC| encountered. The Region *R0-R1* boundary is parallel to the Z_{SM} axis, the Region *R1-R2* boundary passes through the Y_{GSM} axis, and the Region *R2-R3* boundary is parallel to the Z_{GSM} axis. As ψ changes sign from positive to negative the neutral sheet in the magnetotail shifts from above to below the GSM equatorial plane by an amount related to the "hinging" distance *HD* and the angle ψ. Meanwhile, the neutral sheet on the dayside remains aligned with the SM equatorial plane and is displaced in the opposite sense. We now define of the neutral sheet-oriented coordinates *X', Y',* and *Z'* in each of the four regions.

Region R0: In Region *R0*, the coordinates *Z'* and Z_{SM} are equivalent while *X'* is aligned with and varies along the X_{SM} axis as a function of the difference between ψ and ψ', namely

$$X' = \frac{X'_{SM}}{\cos(\psi - \psi')} \quad \text{and} \quad Z' = Z_{SM} \tag{3}$$

such that the SM' and SM coordinates are equivalent at $Y_{GSM} = 0$ where we define $\psi = \psi'$.

Region R1: In Region *R1*, the X' coordinate is defined as in Region *R0* but the Z' coordinate is modified to account for this region's wedge shape and written as

$$X' = \frac{X'_{SM}}{\cos(\psi - \psi')} \quad \text{and} \quad Z' = \frac{Z_{SM}}{\cos(|\psi - \psi'| - \theta)} \tag{4}$$

where θ is the angle between the Region *R1-R2* boundary and the point of interest in Region *R1* measured about the point (XC, ZC). This provide a smooth transition in Z' across the Region *R0-R1* boundary where $\theta = |\psi - \psi'|$.

Region R2: Circular arcs measured about (XC, ZC) are used to define constant Z' contours such that the zero contour passes through the GSM origin at the earthward boundary of Region *R2*. The Region *R2-R3* boundary is the vertical line where $X_{GSM} = XC$. If R_C is the distance from (XC, ZC) to some point of interest (X_{GSM}, Z_{GSM}) in Region *R2*, then a point (X_{12}, Z_{12}) on the Region *R1-R2* boundary with the same Z' value has the coordinates

$$X_{12} = XC + \frac{\psi'}{|\psi'|} R_C \sin\psi'$$

$$\tag{5}$$

$$Z_{12} = ZC + \frac{\psi'}{|\psi'|} R_C \cos\psi'$$

Our Region R2 neutral sheet-oriented coordinates can then be written as

$$X' = -R_C \cos^{-1}\left[1.0 - 0.5\left(\frac{\left\{(X_{GSM} - X_{12})^2 + (Z_{GSM} - Z_{12})^2\right\}^{1/2}}{R_C}\right)^2\right]$$

$$\tag{6}$$

$$Z' = \frac{\psi'}{|\psi'|}\left(R_C - |HD\sin\psi' - ZC|\right)$$

where X' is the distance, measured along a circular arc of radius R_C, between the Region *R1-R2* boundary point (X_{12}, Z_{12}) and any Region *R2* point (X_{GSM}, Z_{GSM}). We see that X' is always negative in Region *R2* while Z' is positive above and negative below the neutral sheet.

Region R3: The Region R3 system becomes rectilinear and its coordinates are written as

$$X' = -\left|(Z_{GSM} - ZC)\psi'\right| - XC + X_{GSM}$$

(7)

$$Z' = Z_{GSM} - HD \sin \psi'$$

The coordinate X', measured tailward from the Region $R1$-$R2$ boundary, incorporates an appropriate arc length from Region $R2$ and a straight portion tailward of $X_{GSM} = XC$ while Z' is measured along the Z_{GSM} direction relative to the neutral sheet position.

The Coordinate Y': Our new coordinate Y' depends on the value of Y_{GSM}, the "hinging" distance HD, and the dipole tilt angle ψ. We integrate Eq. (2) to get the length along the curve it defines in the GSM Y-Z place between $Y_{GSM} = 0$ and the point of interest and get

$$Y' = \frac{Y_{GSM}}{2\chi}\left\{\chi\left(1 + \chi^2\right)^{1/2} + \ln\left[\chi + \left(1 + \chi^2\right)^{1/2}\right]\right\} \qquad \text{for } |Y_{GSM}| < 13.86 \text{ Re}$$

(8)

$$\text{where} \quad \chi = \left(1.4391534 \times 10^{-2}\right)(HD)(Y_{GSM}) \sin \psi$$

When outside the indicated range we get Y' by evaluating (8) at $Y_{GSM} = \pm13.86$ Re, as appropriate, and adding a length equal to $\left(|Y_{GSM}| - 13.86\right)$ Re owing to the linear flank portion. This flattening of the neutral sheet in the outer magnetotail flanks will not significantly affect magnetic field mappings as the observed neutral sheet deviates only slightly (in the opposite sense from the midnight deflection) from the GSM equatorial plane in that region.

2.3. Dependence on Magnetic Activity

The coordinate geometry described above requires knowledge of the neutral sheet "hinging" distance HD which is the geocentric distance measured along the negative SM x-axis characterizing the neutral sheet's displacement from the $Z_{GSM} = 0$, namely $\Delta z = HD \sin \psi$. As noted above, most neutral sheet models have adopted the use of a single average value for HD and thus are incapable of representing shifts related to variations in cross-tail current strength and distribution. In magnetic field models, for example, it can easily be shown that decreasing the cross-tail current density increases the relative influence of the tilting main field so the neutral sheet is displaced farther from the equatorial plane. As reviewed briefly by *Fairfield* [1980], observations clearly indicate the tendency for the neutral sheet to be closer to the GSM equatorial during magnetically active times (when the cross-tail current density is larger on average). This

8

implies that our coordinate system geometry would benefit if HD were dependent on magnetic activity, i.e., if we had $HD = HD(Kp)$.

As a guide, we will use the relationship *Lopez* [1990] determined using AMPTE/CCE magnetic field data from the nightside region between R = 5 and 8.8 Re, namely

$$MLAT = -(0.14Kp + 0.69)[\cos\Phi]^{1/3}(0.065R^{0.8} - 0.16)\psi \tag{9}$$

where $MLAT$ is the position in degrees of the neutral sheet relative to the SM equator, Kp is the magnetic activity index, Φ is the magnetic local time in degrees ($\Phi = 0$ at midnight), R is geocentric radius in Re, and ψ is the dipole tilt angle in degrees. Eq. (9) describes a neutral sheet that diverges increasingly from the SM equatorial plane as each of the variables Kp, R, and ψ increase in magnitude while the neutral sheet converges with the equatorial plane at both dawn and dusk. This latter feature supports our selection of the SM equatorial plane for the neutral sheet position on the dayside.

An expression for HD as a function of Kp was derived by comparing the neutral sheet position estimates given by Eq. (9) with those of our new coordinate system. Using a large dipole tilt angles of $\psi = \pm 34°$, the neutral sheet position given by (9) was determined for the full range of Kp values ($Kp = 0.0$ to 9.0 by 0.3333) and R values ($R = 5.0$ to 8.8 Re by 0.1 Re) at midnight. The equivalent coordinates in our new neutral sheet oriented coordinate system are found and the error between the two methods is represented by the magnitude of our new Z' coordinate as ideally the Z'=0 surface coincides with the neutral sheet. The linear function minimizing the error is given by the upper expression of the following equation used for the entire Kp range.

$$HD = (-0.86)Kp + 13.36667 \quad \text{for} \quad 0.0 \le Kp \le 6.0$$
$$\tag{10}$$
$$HD = 8.20667 \quad \quad\quad \text{for} \quad Kp > 6.0$$

where the "hinging" distance HD is in Re and ranges from approximately 13.4 to 5.6 Re as Kp increases from values 0.0 to 9.0. The maximum error (given by $\overline{|Z'|}$), occurring for the extreme Kp values of 0.0 and 9.0, is 0.133 Re while the average error approaches zero (0.0004 Re) for a value of Kp very close to 3.33 (or 3+) when HD equals its nominal value of 10.5 Re. The average overall error is 0.086 Re for this $\psi = \pm 34°$ case, is half as large when $\psi = \pm 19°$, and vanishes as expected when $\psi = 0°$. Because GSM input is restricted to $|Z_{GSM}| < ZO$ and $Z0$ depends on the value of HD (relationship not shown here) we must restrict use of the above linear relationship to Kp values less than 6.0 in order to allow $|Z_{GSM}|$ input values of up to $Z0 = 17$ Re. This

modification introduces some additional error *only in the high Kp range* but increases the overall average error from 0.048 to 0.068 Re at midnight for the $\psi = \pm 19°$ case. *Fairfield* [1980] notes that there are no large changes in erroneous neutral sheet prediction when our range of *HD* values, 8.2 to 13.4 Re, is used. We note that while the error has been minimized at midnight and is, by design, zero at dawn and dusk, the average error between our neutral sheet model and Eq. (9) peaks at 0.13 Re near MLT values of 5 and 19 for the $\psi = \pm 19°$ case. These differences are related to the Y_{GSM} dependence of the ellipse used to describe the far-tail neutral sheet position.

3. Examples

Figures 2 to 39 show neutral sheet-oriented coordinate (X', Y', Z') grids plotted in various X-Z and Y-Z GSM planes for conditions defined by permutations of a selection of ψ and Kp values (i.e., $\psi = 5$, 20, and 35 degrees and $Kp = 0$, 3, 6). Contours of constant X', Y', and Z' assume the same approximate relation to each other as the straight contours of constant X, Y, Z do in the GSM coordinate system. In each plot, the Earth is represented by a cross at the projected location of the GSM origin. For $\psi = 0$ degrees, the neutral sheet-oriented coordinates becomes equivalent to the GSM coordinates.

In the X_{GSM}-Z_{GSM} grid views (with Sun to the right), the vertices formed by intersecting contour lines remain equidistant as the grid flexes with changing dipole tilt angle, ψ. In Region *R2*, Z' contours form circular arcs centered at the point (XC, ZC) and are tangent to the X'_{SM} direction at the Region *R1-R2* boundary and tangent to the X_{GSM} direction at the Region *R2-R3* boundary. See Figure 1 (with Sun to the left) for Region and boundary definitions. The defined neutral sheet represents the $Z' = 0$ surface such that the constant Z' contour highlighted in Figure 1 has a value $Z' < 0$. The X' coordinate values are positive sunward of the $X'_{SM} = 0$ plane. In Region *R3*, the neutral sheet is displaced in the Z_{GSM} direction by an amount proportional to the neutral sheet "hinging" distance *HD*, which decreases as *Kp* increases. For positive (negative) tilt angles ψ, the displacement is above (below) the GSM equatorial plane.

In the Y_{GSM}-Z_{GSM} views, grid vertices formed by intersecting contour lines are equidistant only for $X_{GSM} < XC$ as contours of constant Y' are defined to be straight lines. Down the magnetotail center, e.g., at $X_{GSM} = -21$ Re, the Z' contours become elliptic as the neutral sheet is displaced above (below) the GSM equatorial plane for positive (negative) ψ values. Moving toward the magnetotail flanks, the neutral sheet approaches and becomes aligned with the GSM equatorial plane. As we move sunward, i.e., from $X_{GSM} = -7$ Re to $+7$ Re, the grid patterns appear more irregular as the selected viewing plane intersects multiple Regions. On the dayside, $Z' = 0$ contours are straight lines in the SM equatorial plane.

4. Comments

The new magnetospheric coordinate system presented here responds to changes in the Earth's dipole tilt angle and the *Kp* index. By tracking the motion of the magnetic neutral sheet as a function of time and geomagnetic activity, it can be used to estimate the relative position of arbitrary points with respect to this magnetic field minimum surface. Accurate knowledge of the neutral sheet's position is important because it greatly influences the shape and tailward extent of magnetic field lines connecting the ionosphere with the plasma sheet. The effectiveness of the MAP3D procedure used to determine energetic particle fluxes for arbitrary locations outside the MSM and MSFM simulation planes is compromised because it does not account for variations in neutral sheet position, i.e., the geomagnetic field configurations it uses fix the tilt angle equal to zero. It is suggested that improved particle flux specifications, owing to more realistic magnetic field mapping assignments to the simulation planes, will result if all future spatial inputs to the MAP3D algorithm are expressed in this new coordinate system rather than in GSM coordinates.

MSM-MAP3D Coordinate System
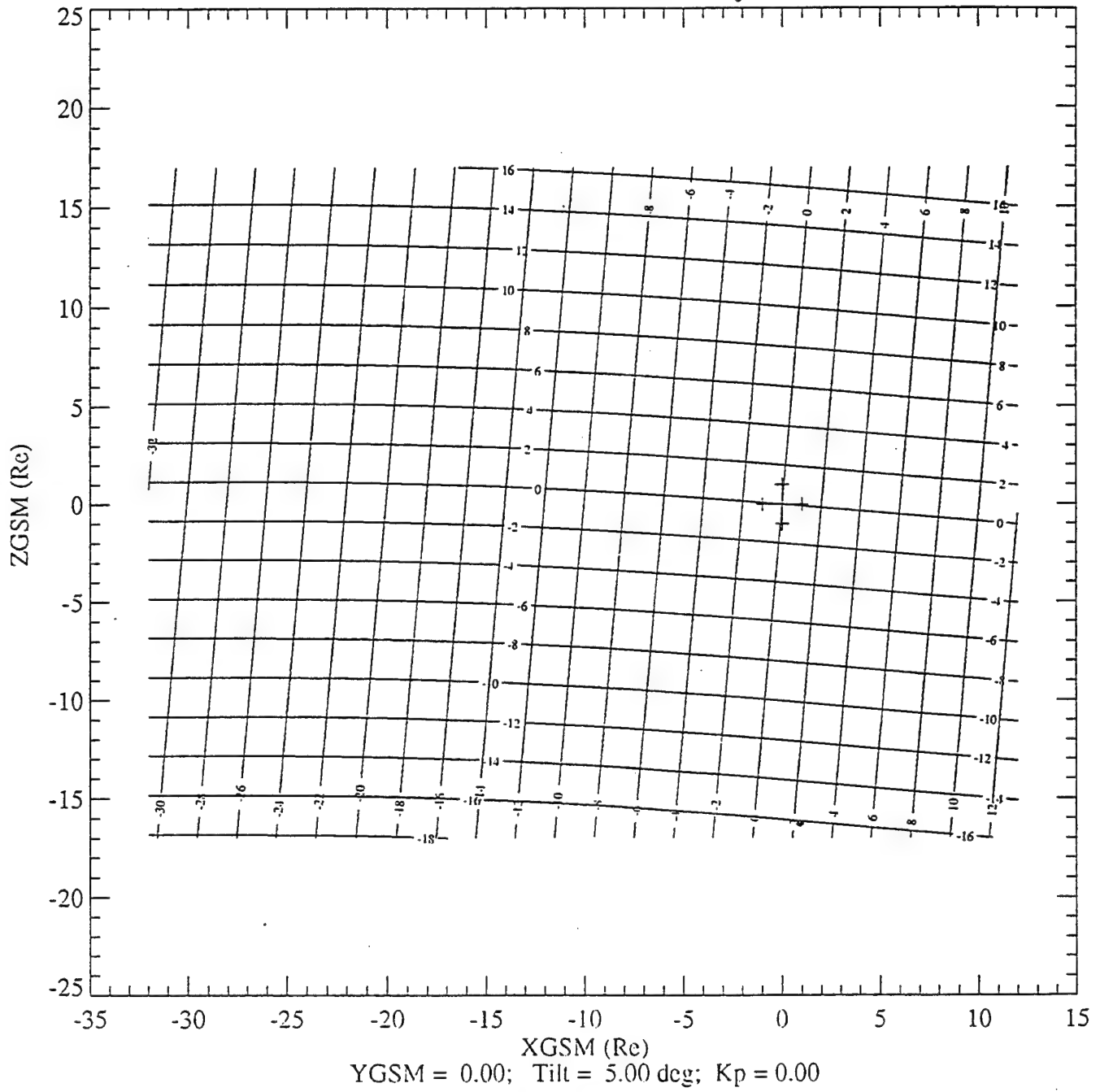
YGSM = 0.00; Tilt = 5.00 deg; Kp = 0.00

FIGURE 2

FIGURE 3

13

MSM-MAP3D Coordinate System

XGSM (Re)

ZGSM (Re)

YGSM = 0.00; Tilt = 35.00 deg; Kp = 0.00
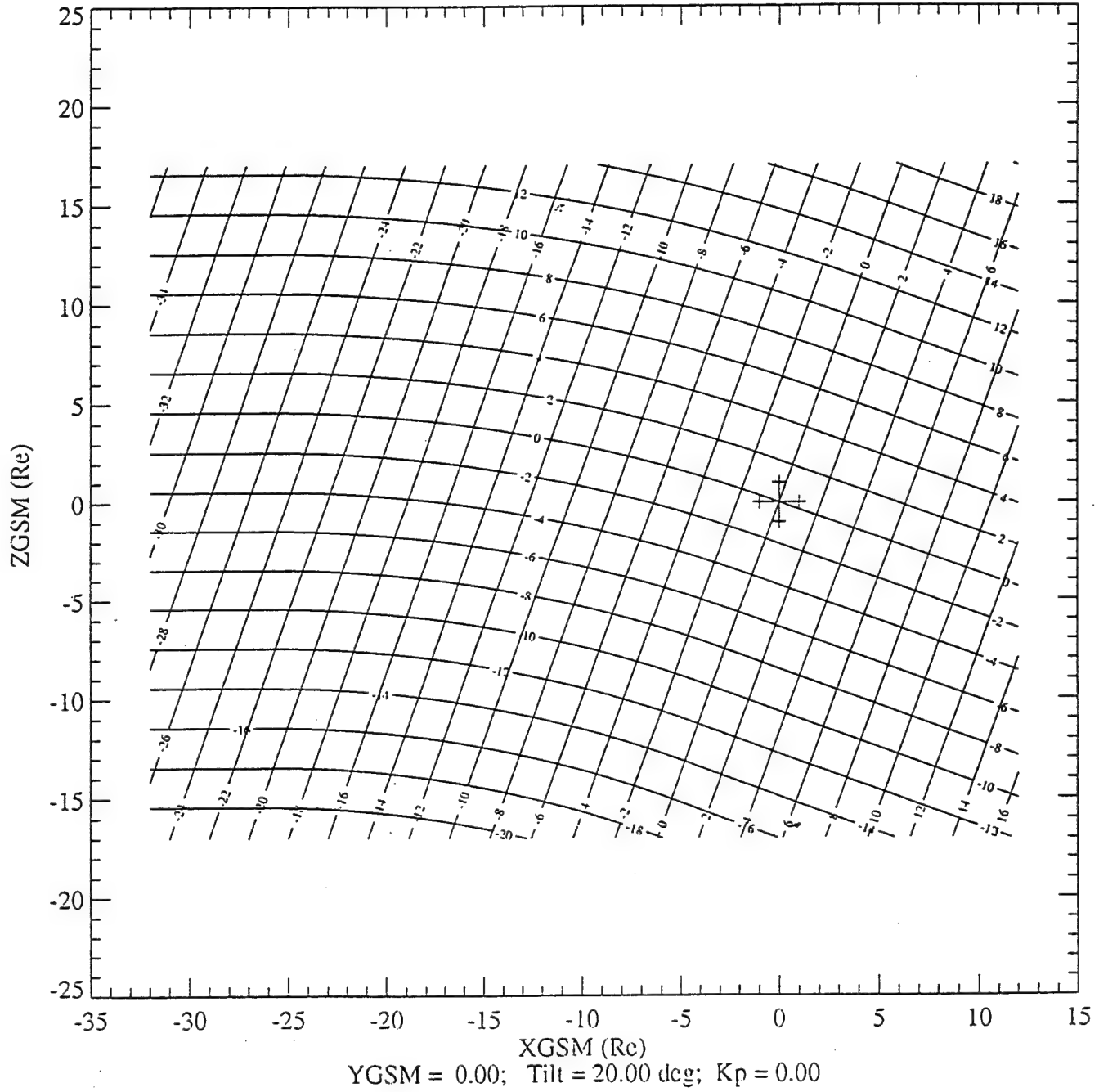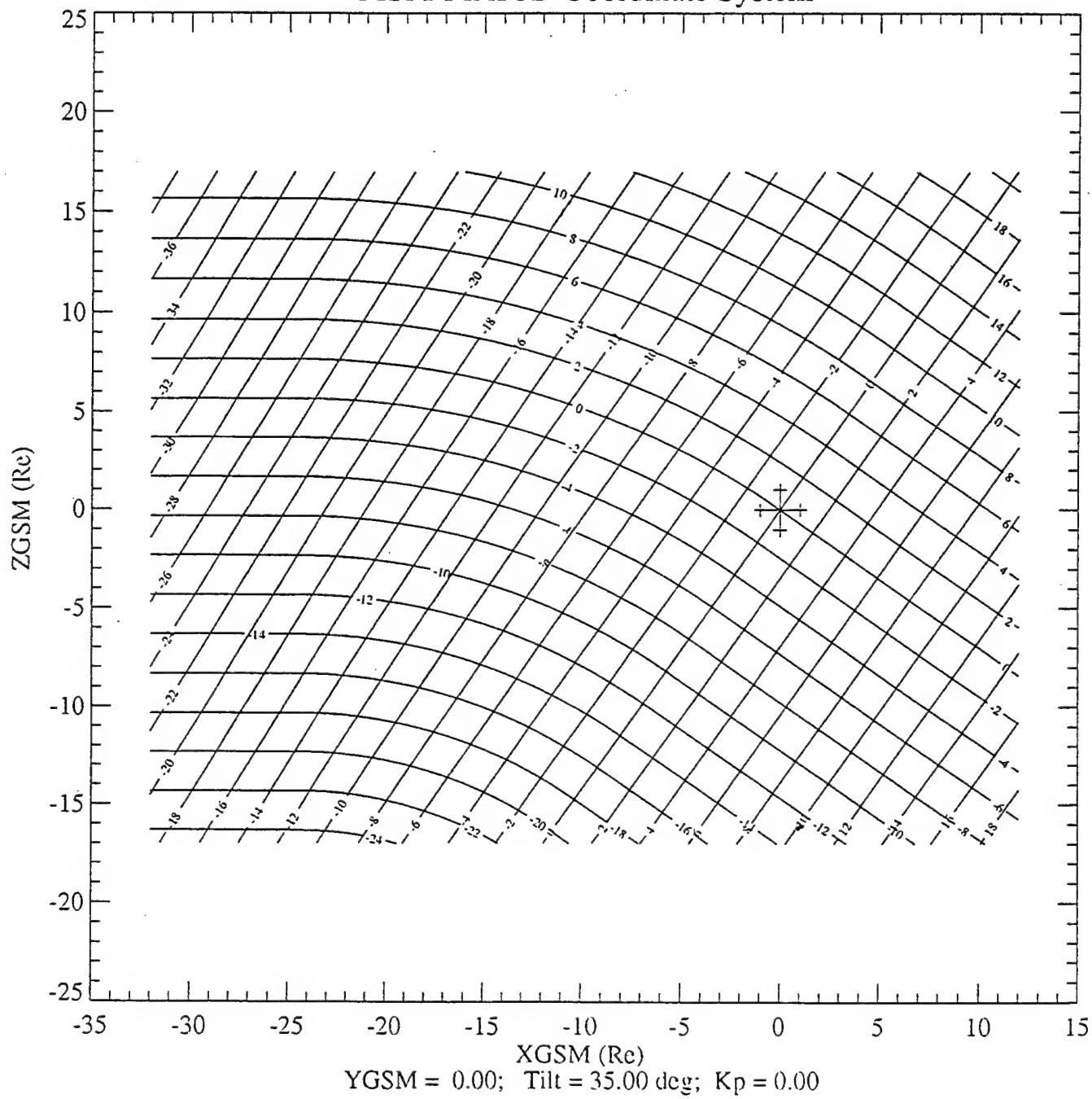
FIGURE 4

MSM-MAP3D Coordinate System

XGSM (Re)

ZGSM (Re)

YGSM =-20.00;   Tilt = 35.00 deg;   Kp = 0.00

FIGURE 5

15
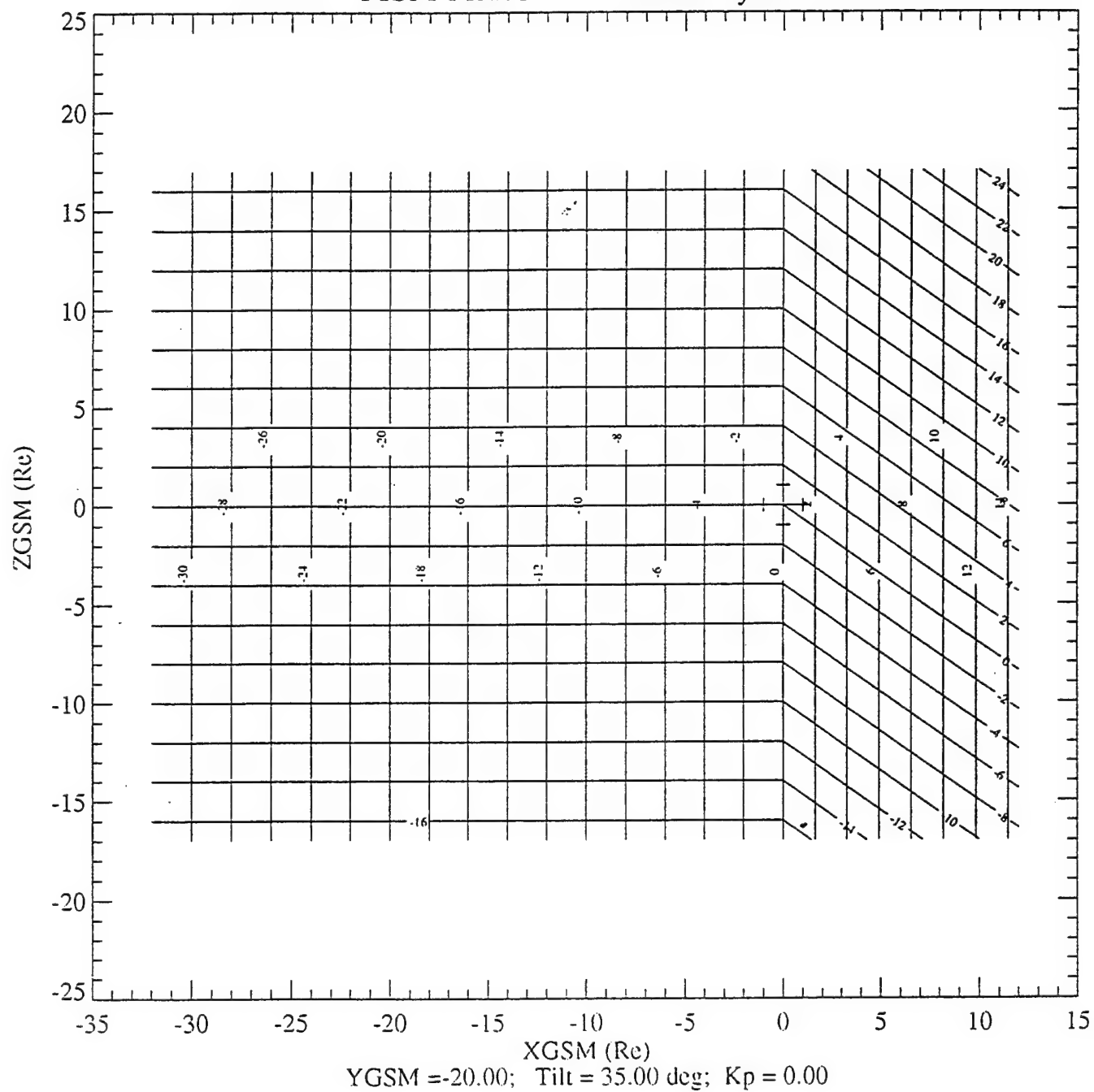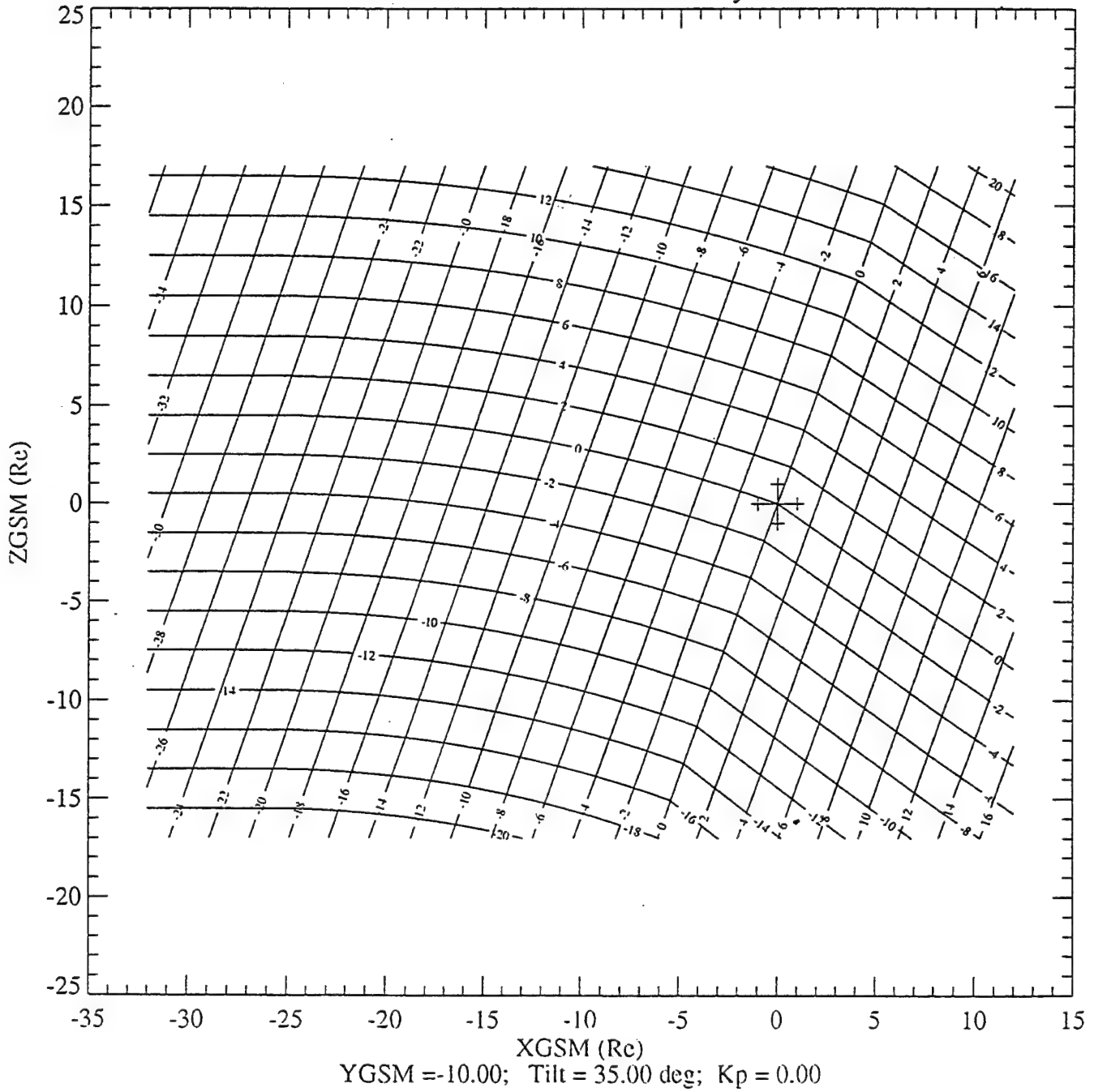
FIGURE 6

MSM-MAP3D Coordinate System

YGSM = 10.00; Tilt = 35.00 deg; Kp = 0.00
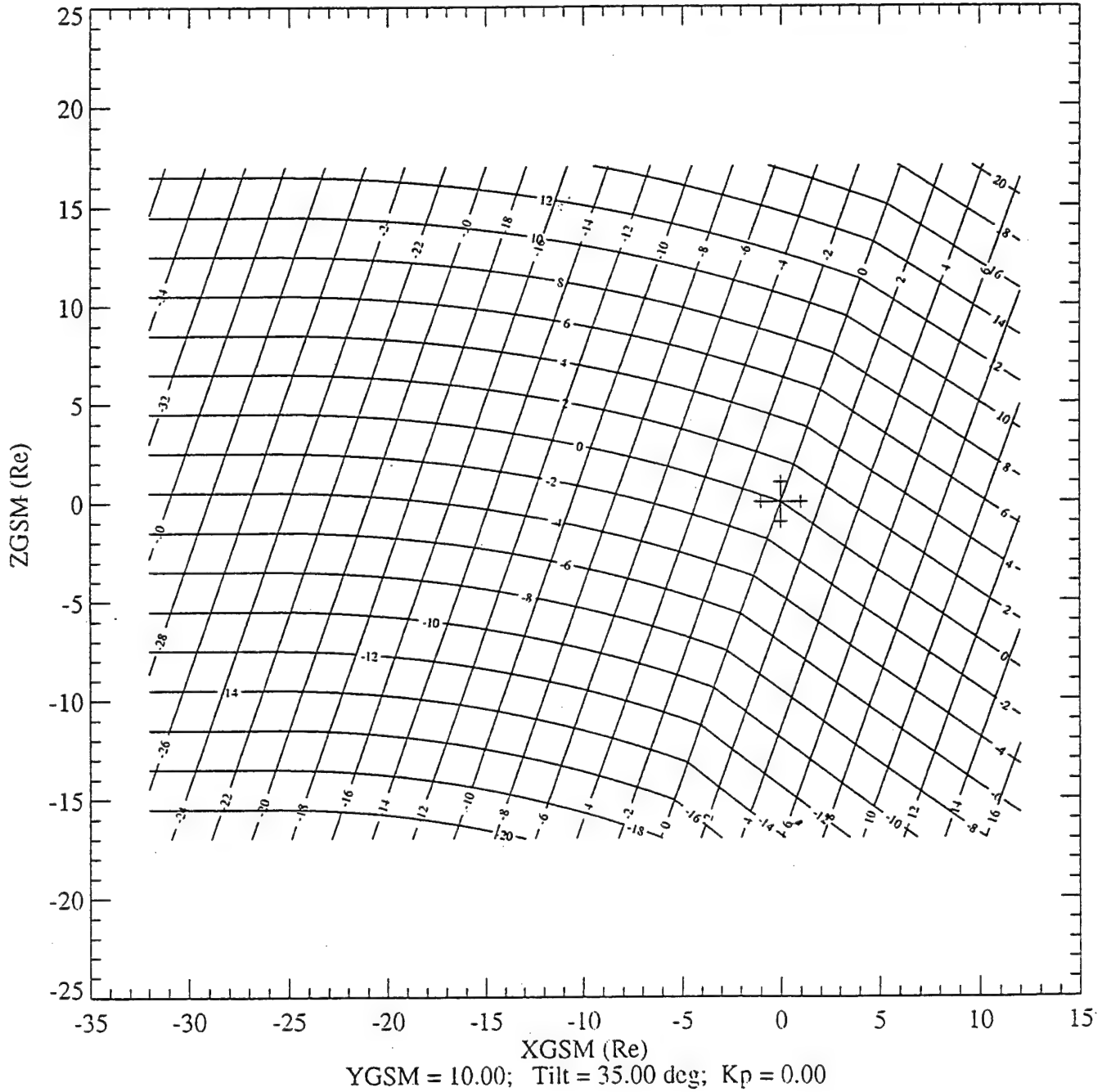
FIGURE 7

MSM-MAP3D Coordinate System

YGSM = 20.00; Tilt = 35.00 deg; Kp = 0.00
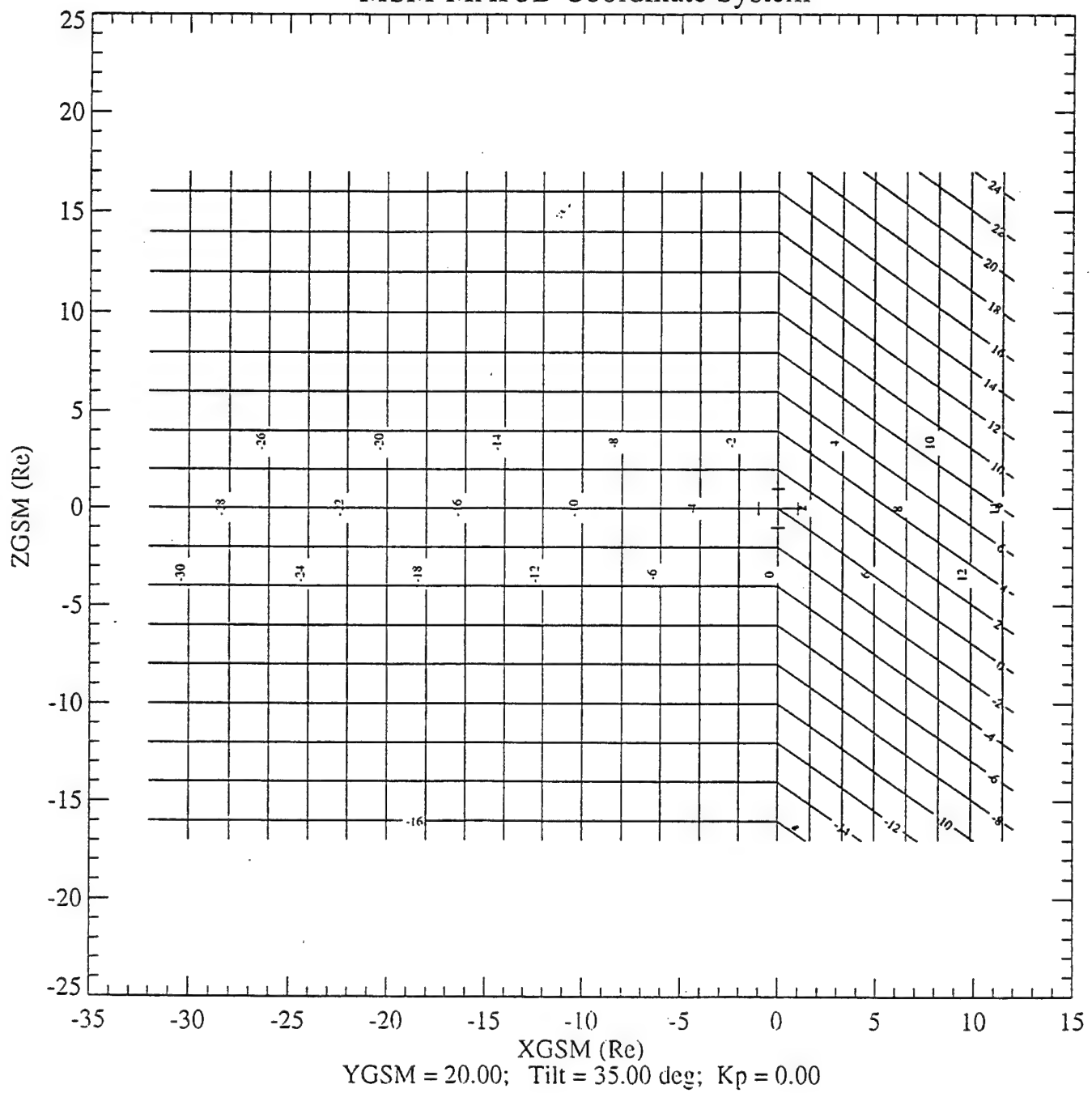
FIGURE 8

MSM-MAP3D Coordinate System
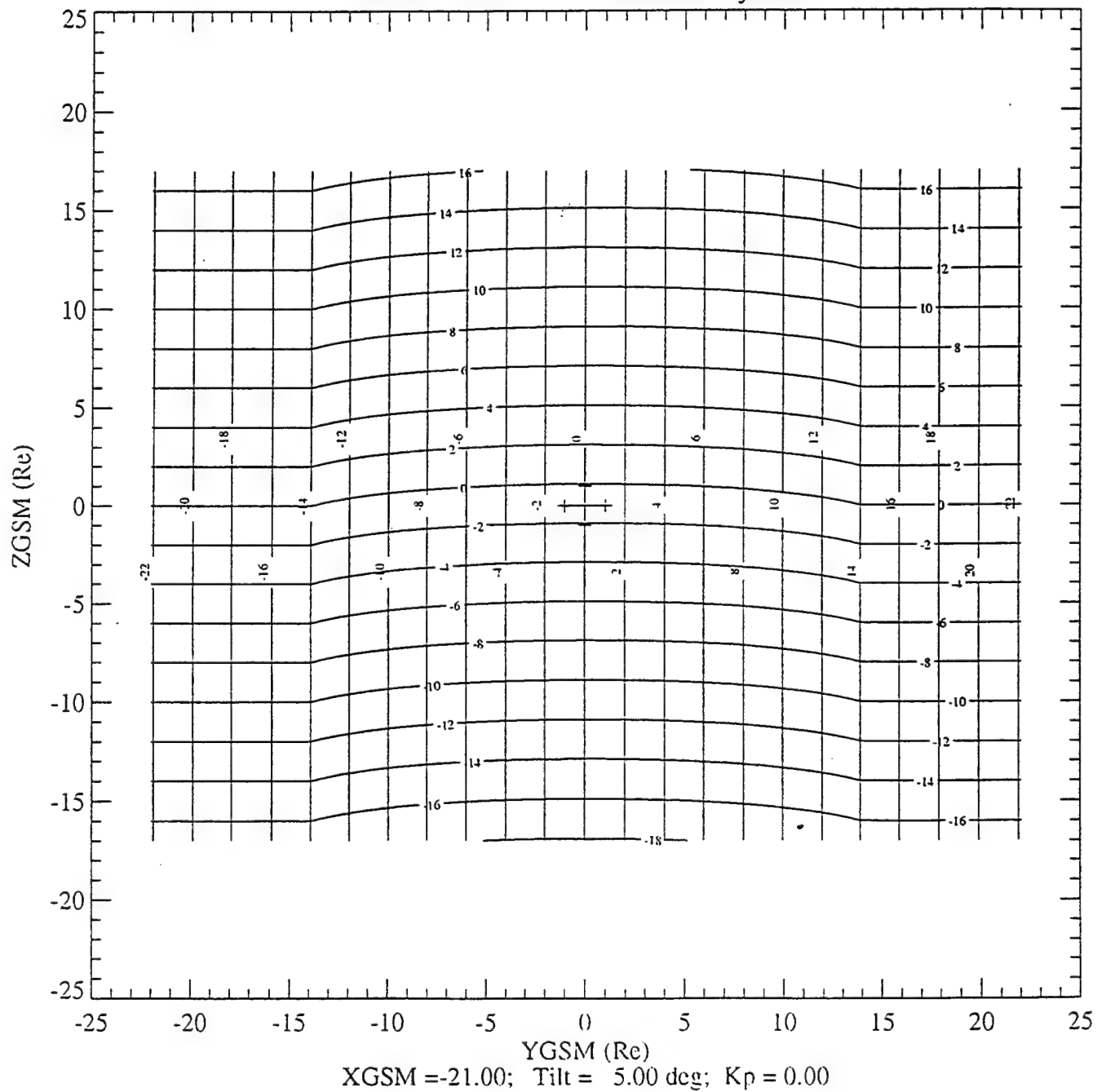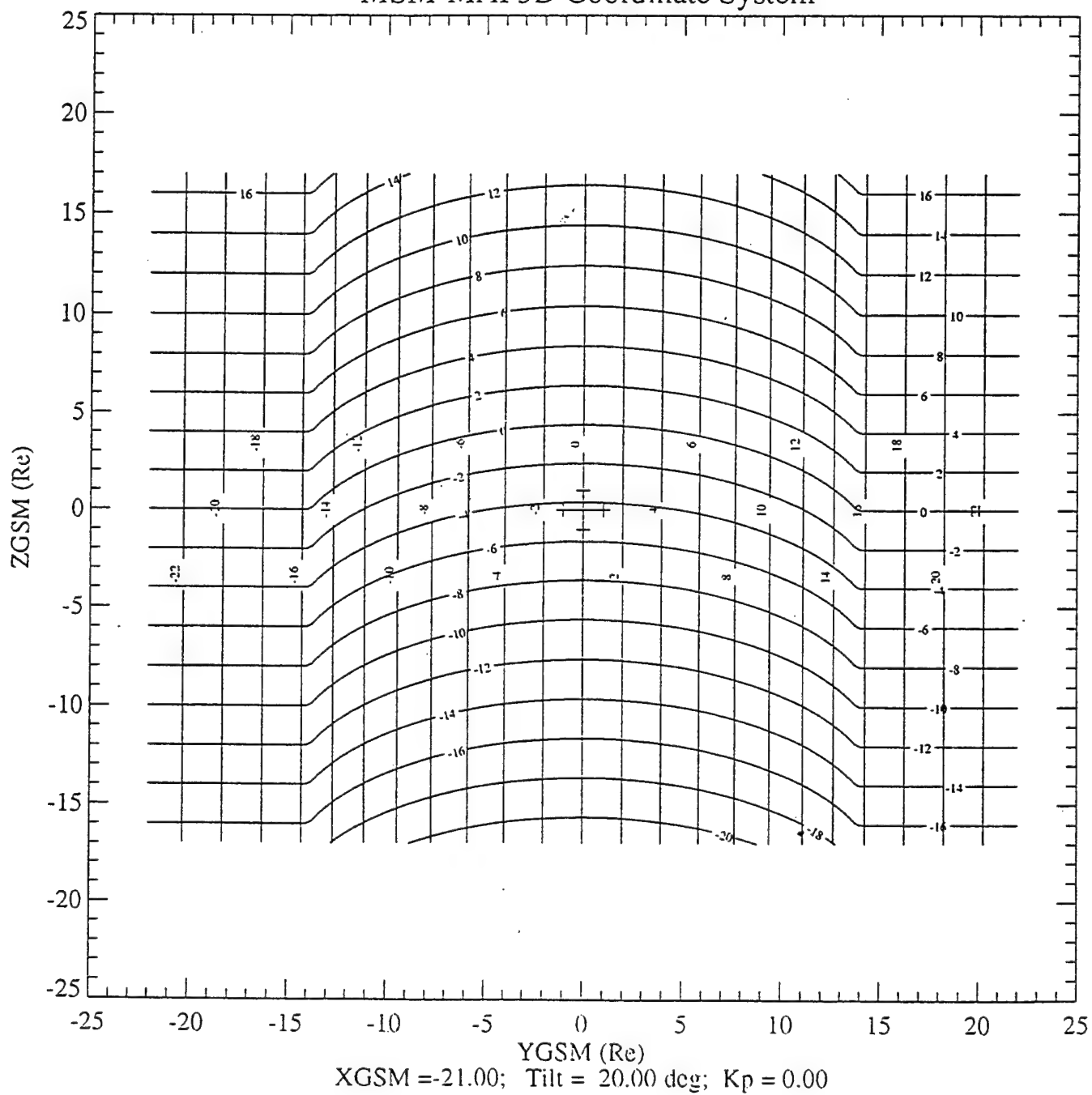
XGSM =-21.00; Tilt = 5.00 deg; Kp = 0.00

FIGURE 9

19

MSM-MAP3D Coordinate System

XGSM =-21.00; Tilt = 20.00 deg; Kp = 0.00

FIGURE 10

20

MSM-MAP3D Coordinate System

YGSM (Re)

XGSM =-21.00;   Tilt = 35.00 deg; Kp = 0.00

FIGURE 11

21

MSM-MAP3D Coordinate System

XGSM =-14.00;   Tilt = 35.00 deg; Kp = 0.00

FIGURE 12

MSM-MAP3D Coordinate System

YGSM (Re)
XGSM = -7.00; Tilt = 35.00 deg; Kp = 0.00

FIGURE 13

23

MSM-MAP3D Coordinate System

XGSM = 0.00; Tilt = 35.00 deg; Kp = 0.00
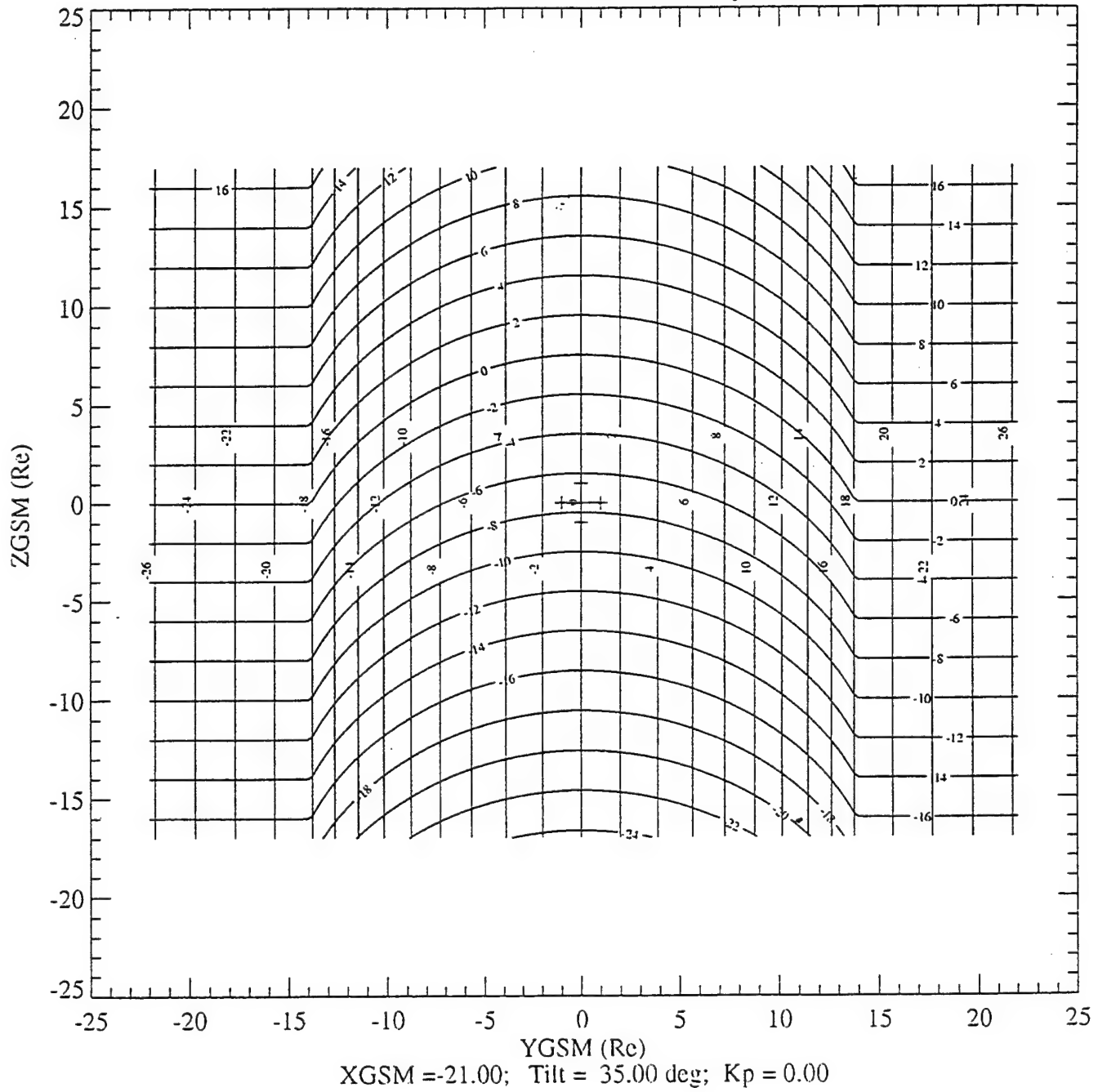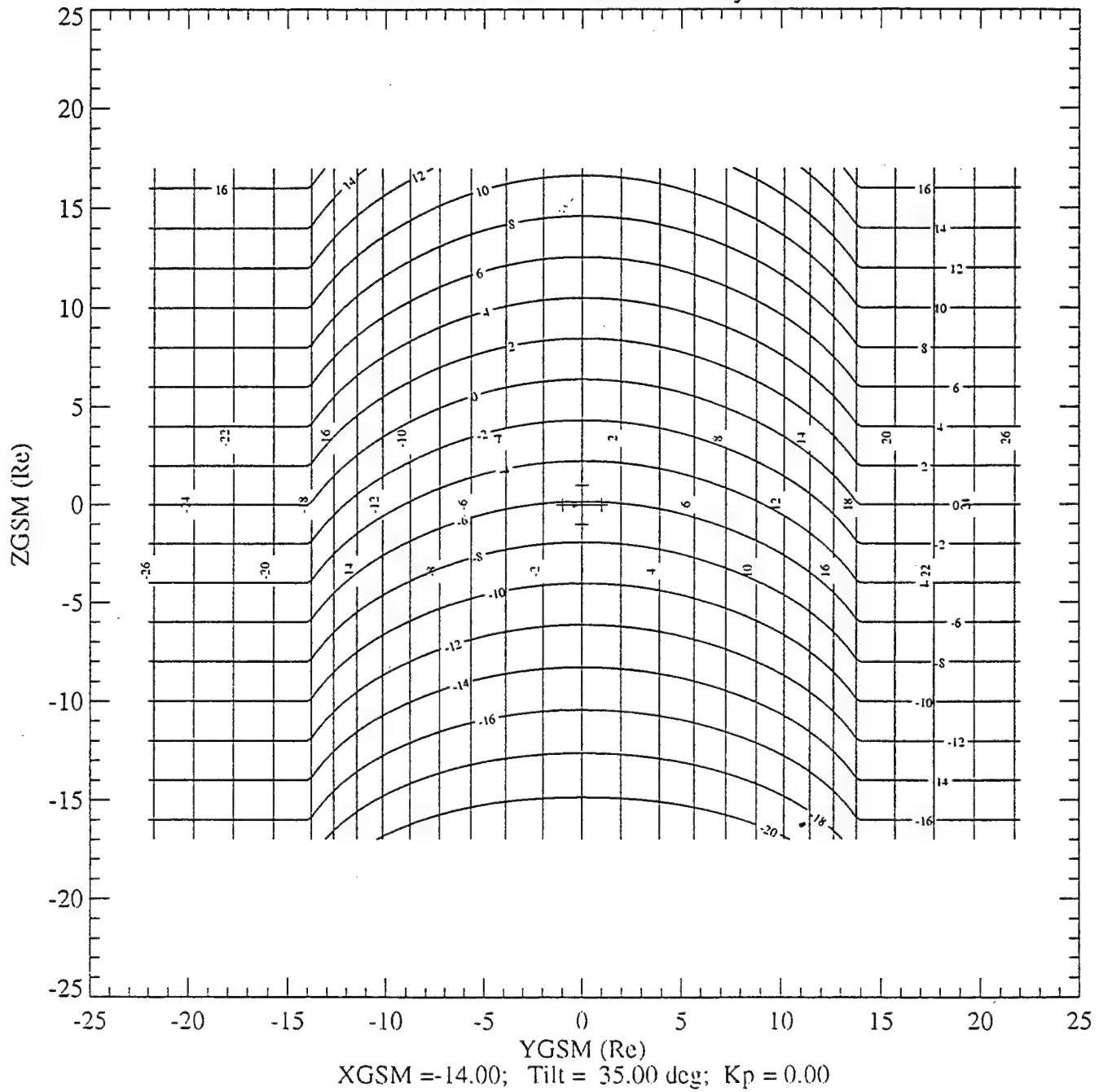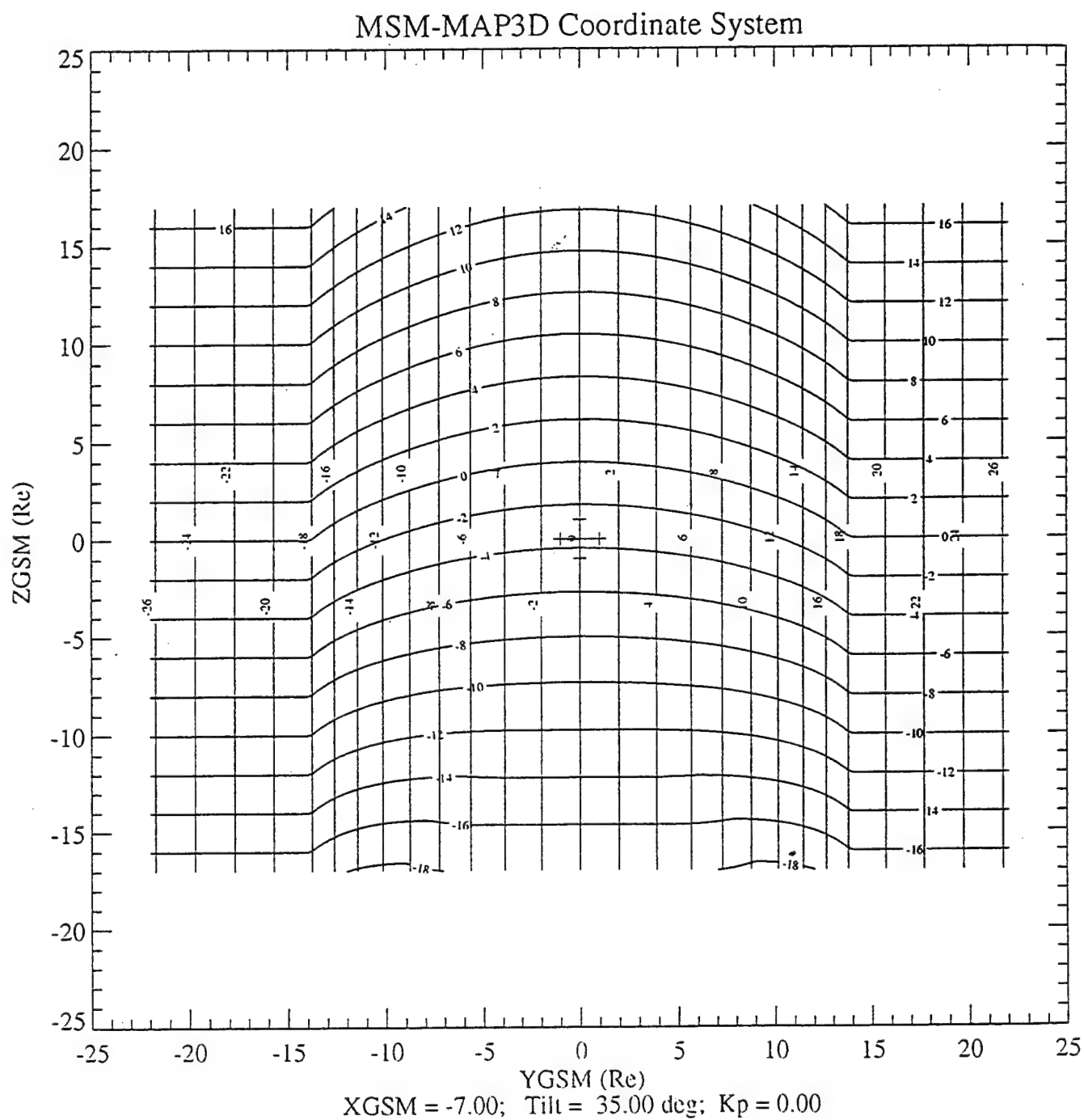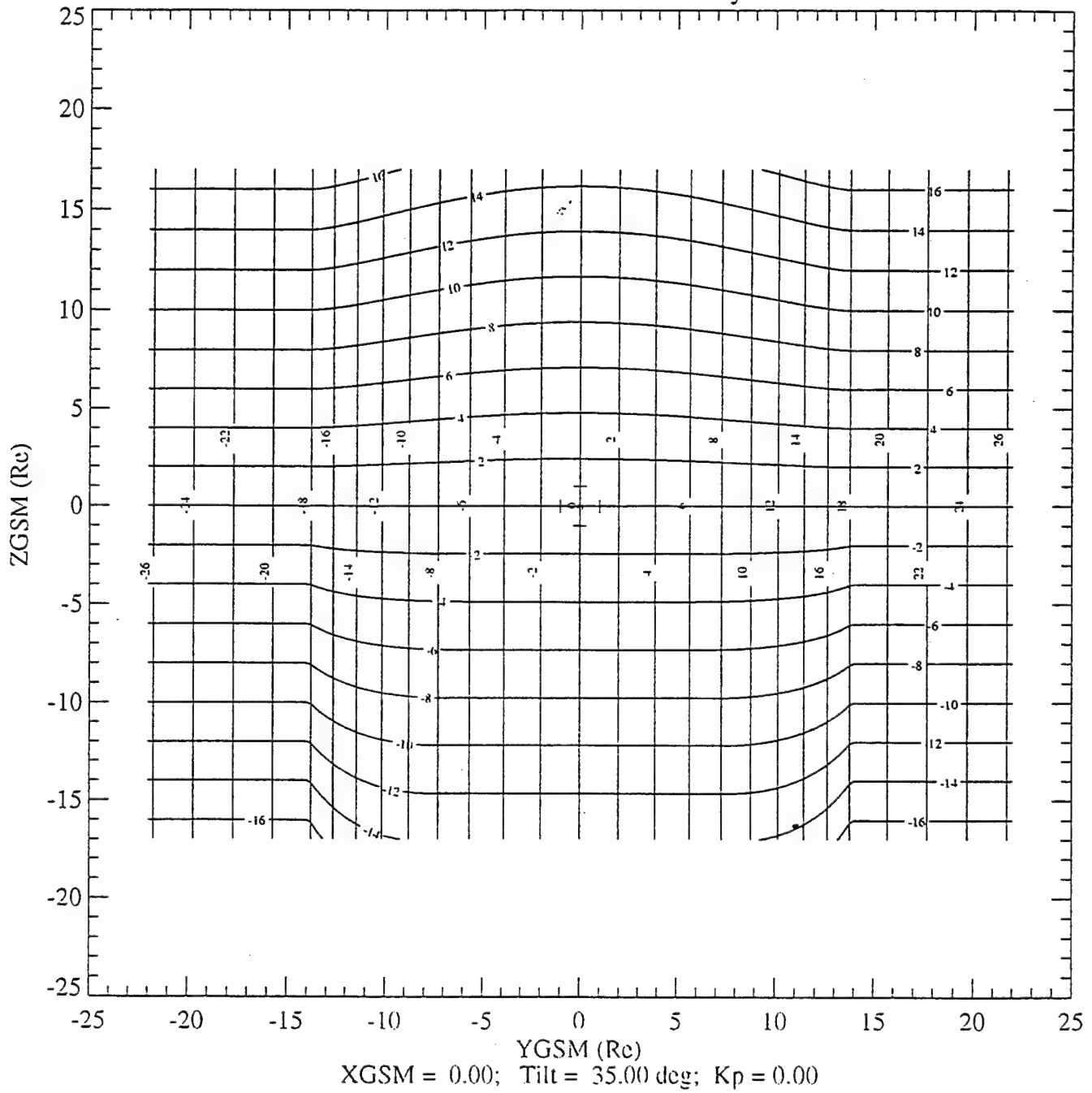
FIGURE 14

MSM-MAP3D Coordinate System

XGSM = 7.00;   Tilt = 35.00 deg; Kp = 0.00
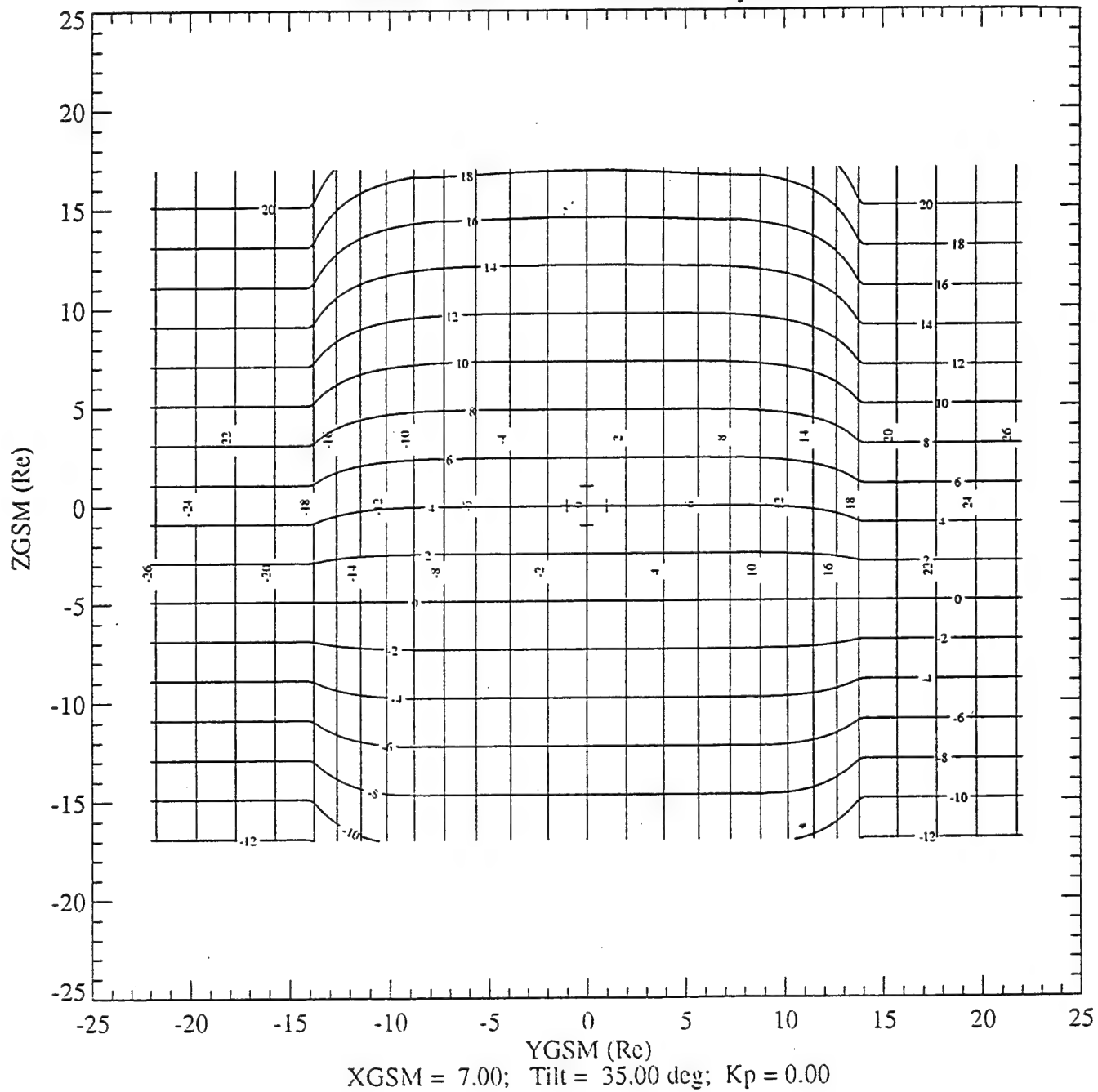
FIGURE 15

MSM-MAP3D Coordinate System

YGSM = 0.00; Tilt = 5.00 deg; Kp = 3.00
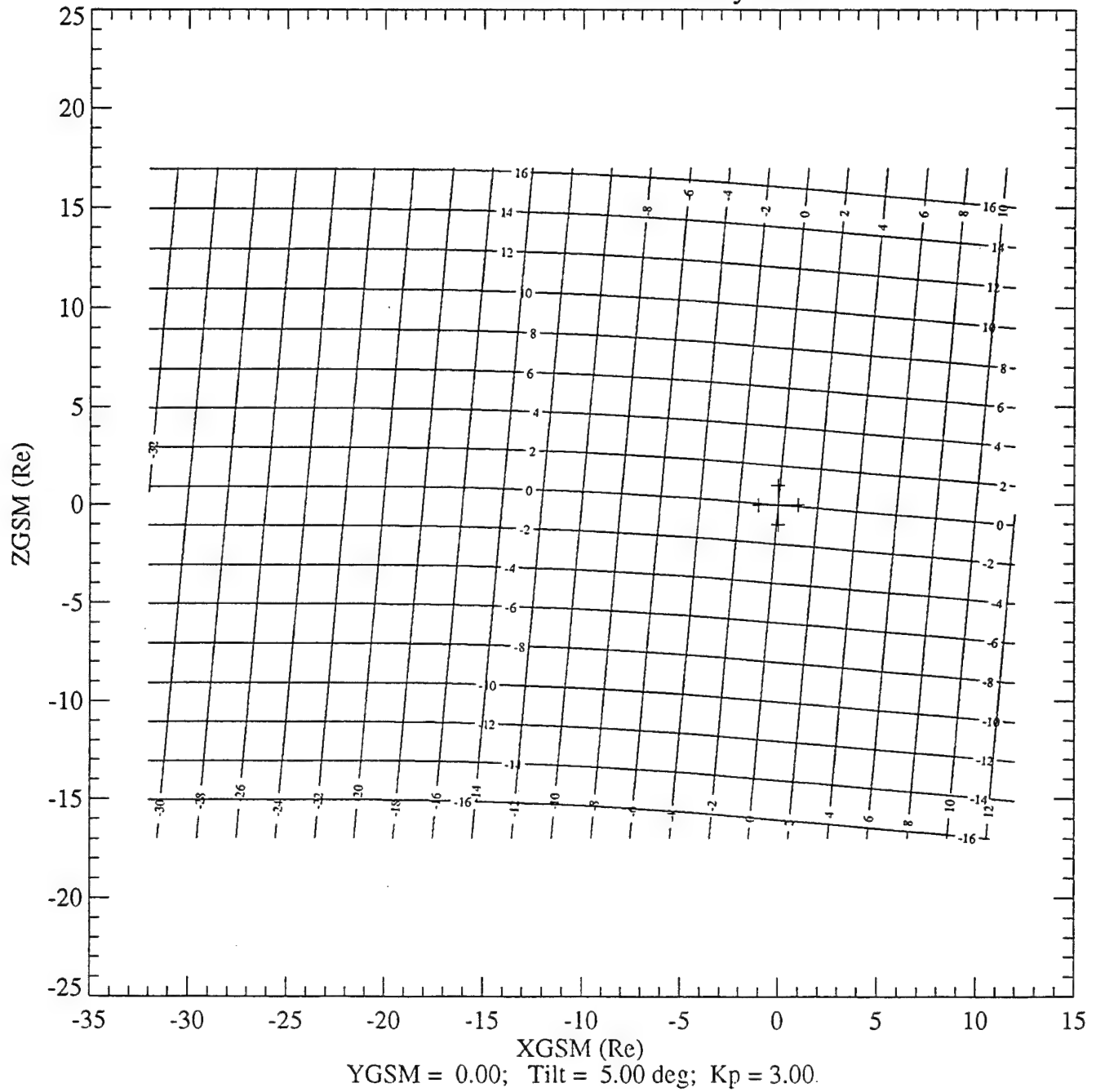
FIGURE 16

MSM-MAP3D Coordinate System

YGSM = 0.00; Tilt = 20.00 deg; Kp = 3.00
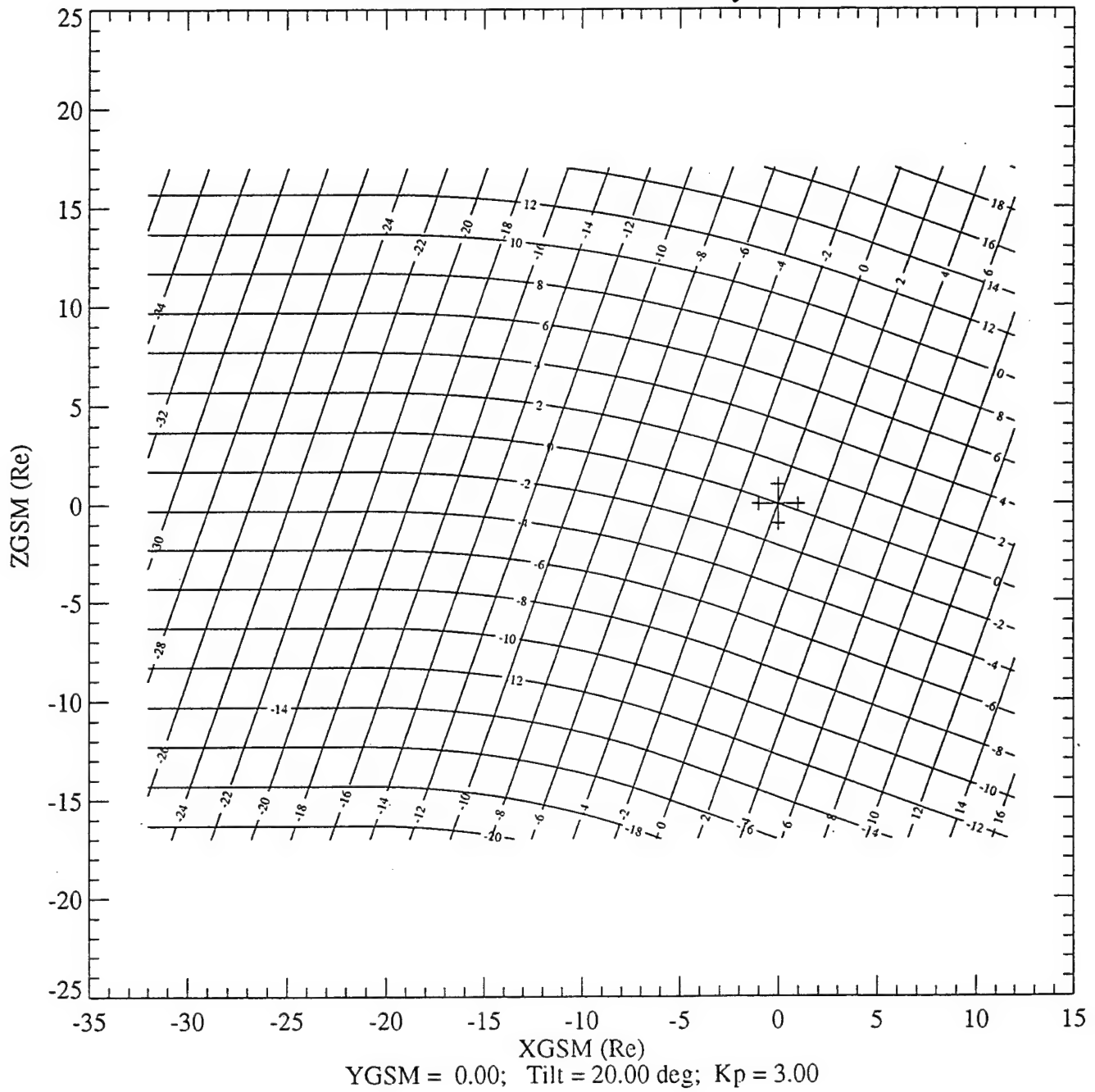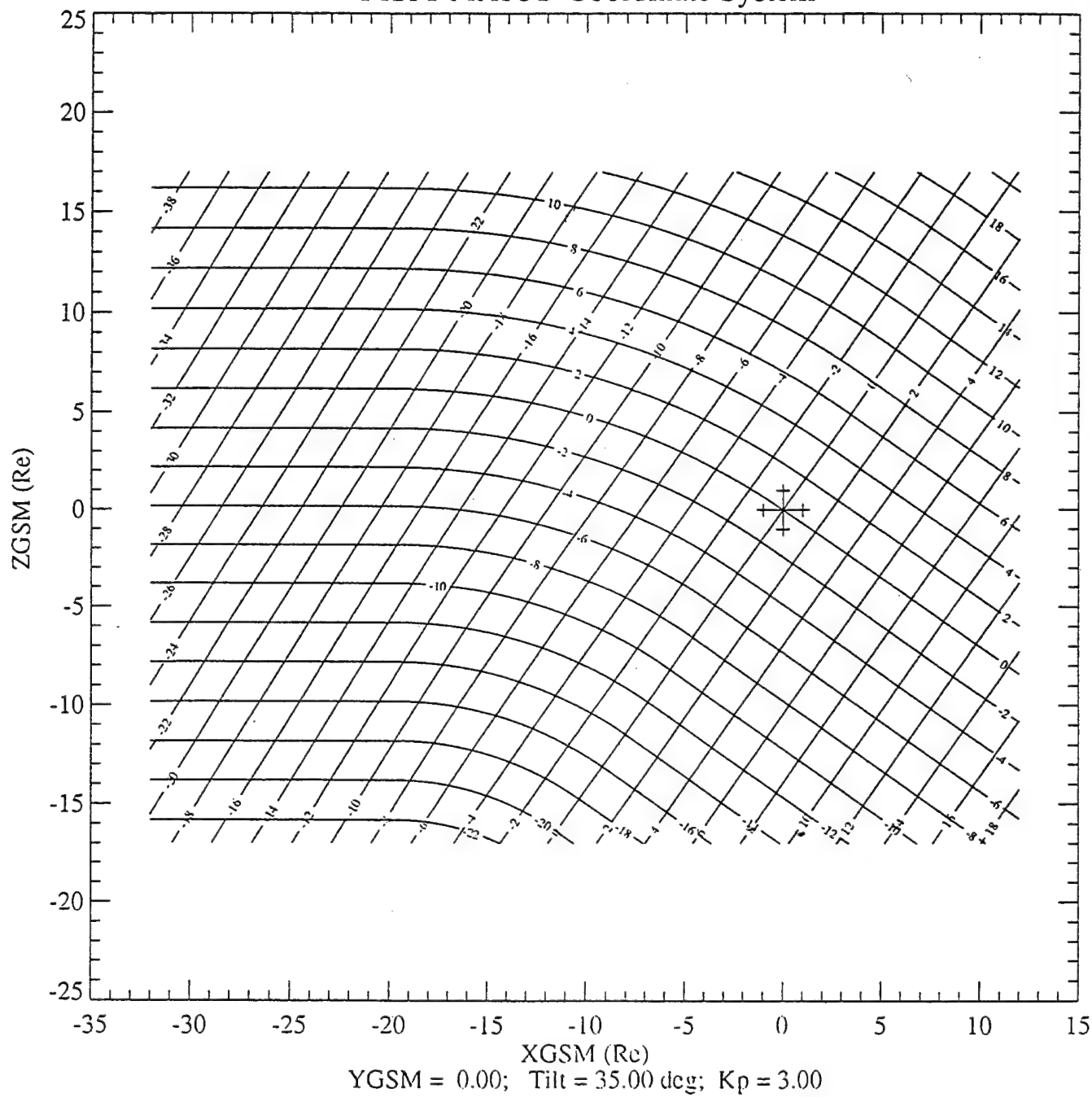
FIGURE 17

FIGURE 18

MSM-MAP3D Coordinate System

YGSM =-20.00; Tilt = 35.00 deg; Kp = 3.00

FIGURE 19

29

MSM-MAP3D Coordinate System

YGSM =-10.00;   Tilt = 35.00 deg;   Kp = 3.00
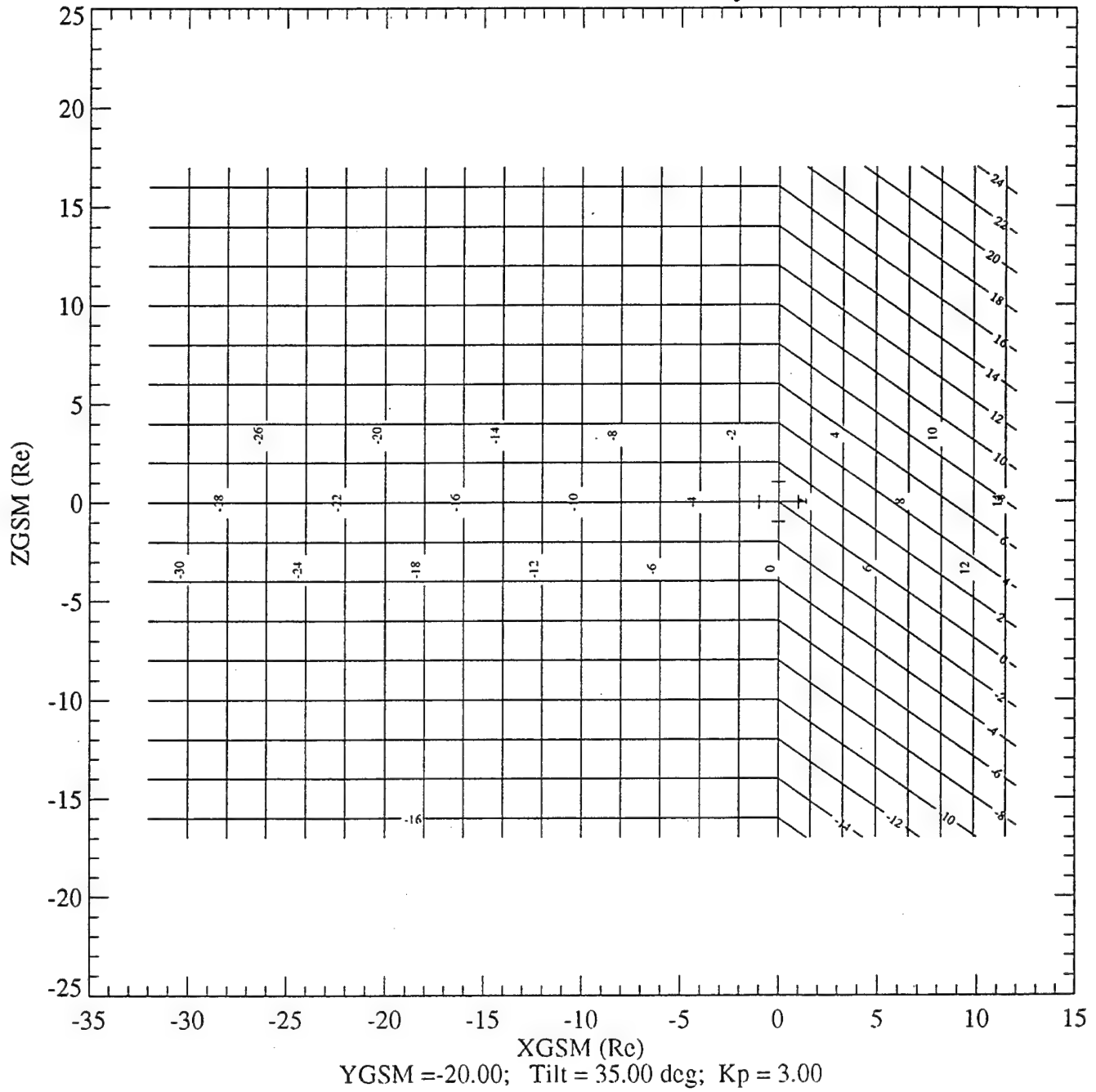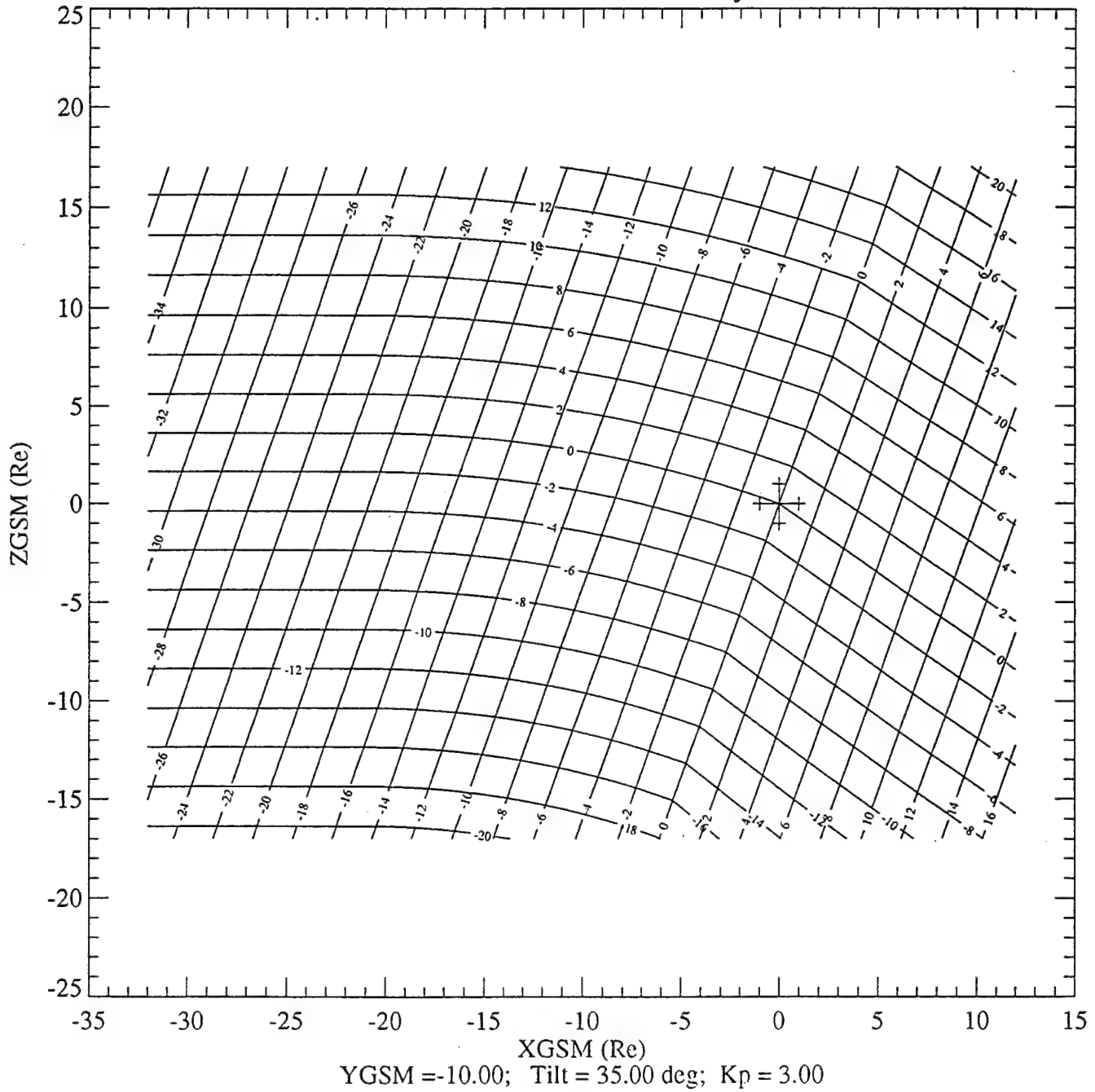
FIGURE 20

MSM-MAP3D Coordinate System

XGSM =-21.00;   Tilt =   5.00 deg; Kp = 3.00

FIGURE 21

MSM-MAP3D Coordinate System

XGSM =-21.00;   Tilt = 20.00 deg; Kp = 3.00
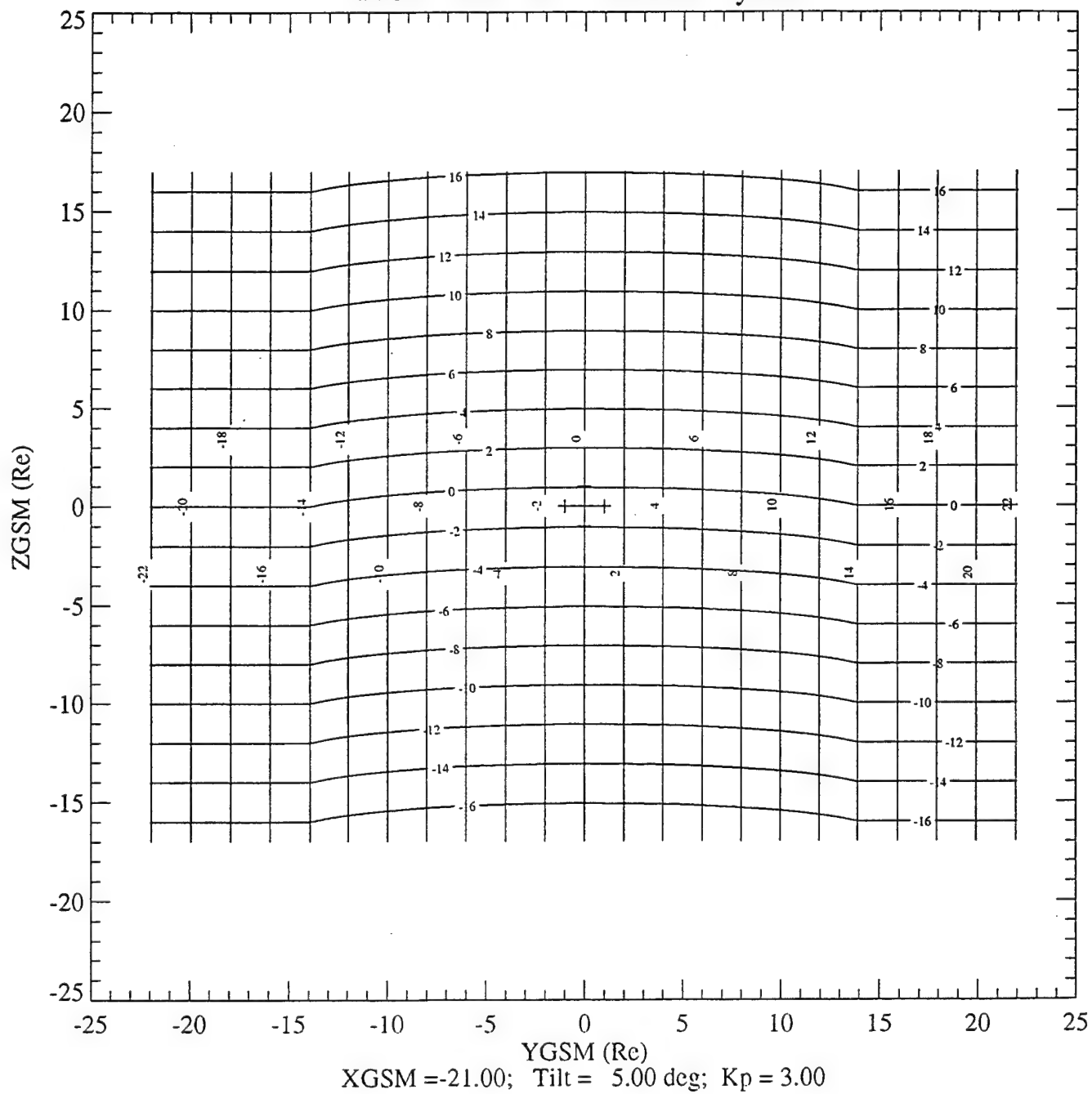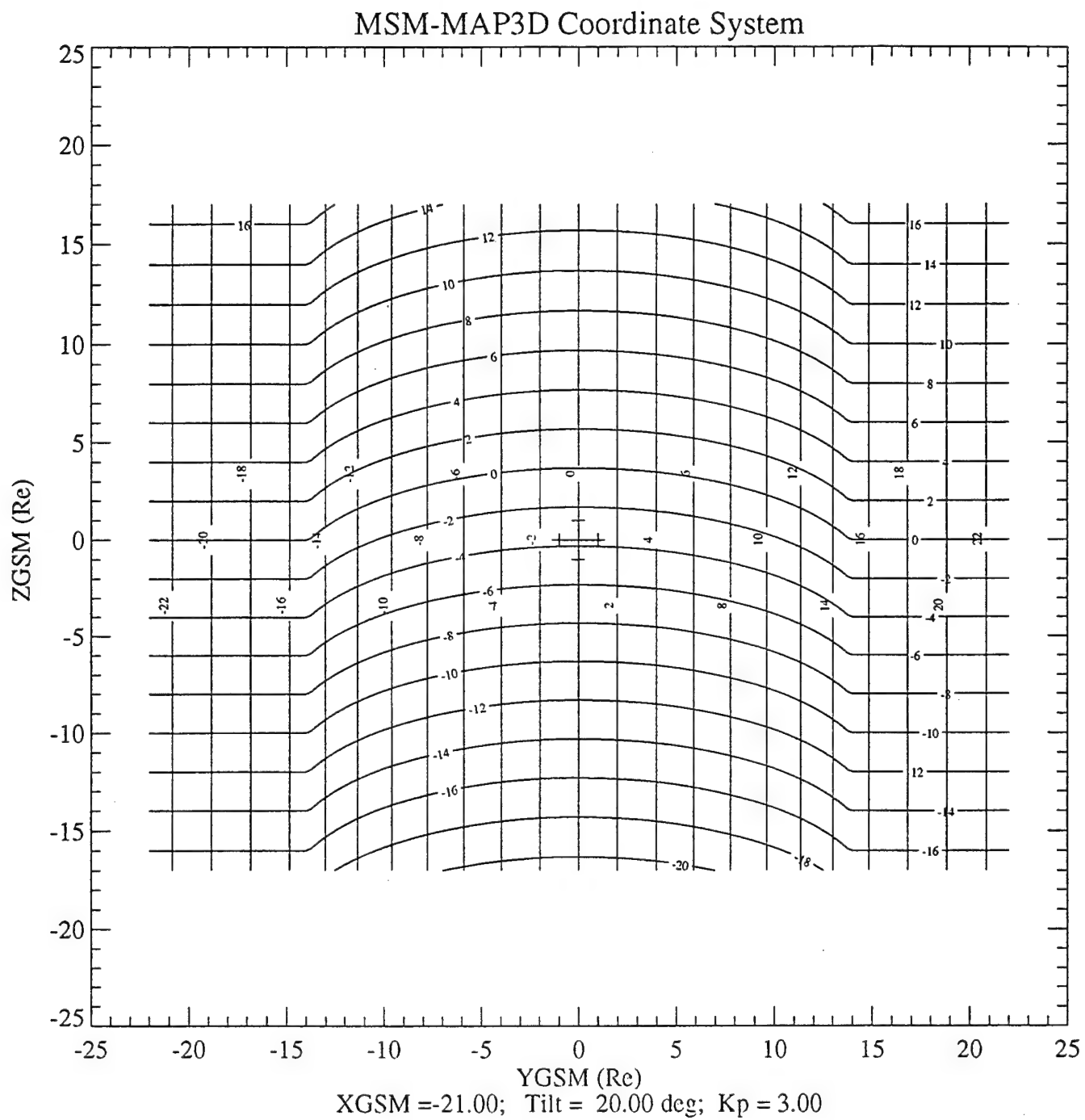
FIGURE 22

MSM-MAP3D Coordinate System
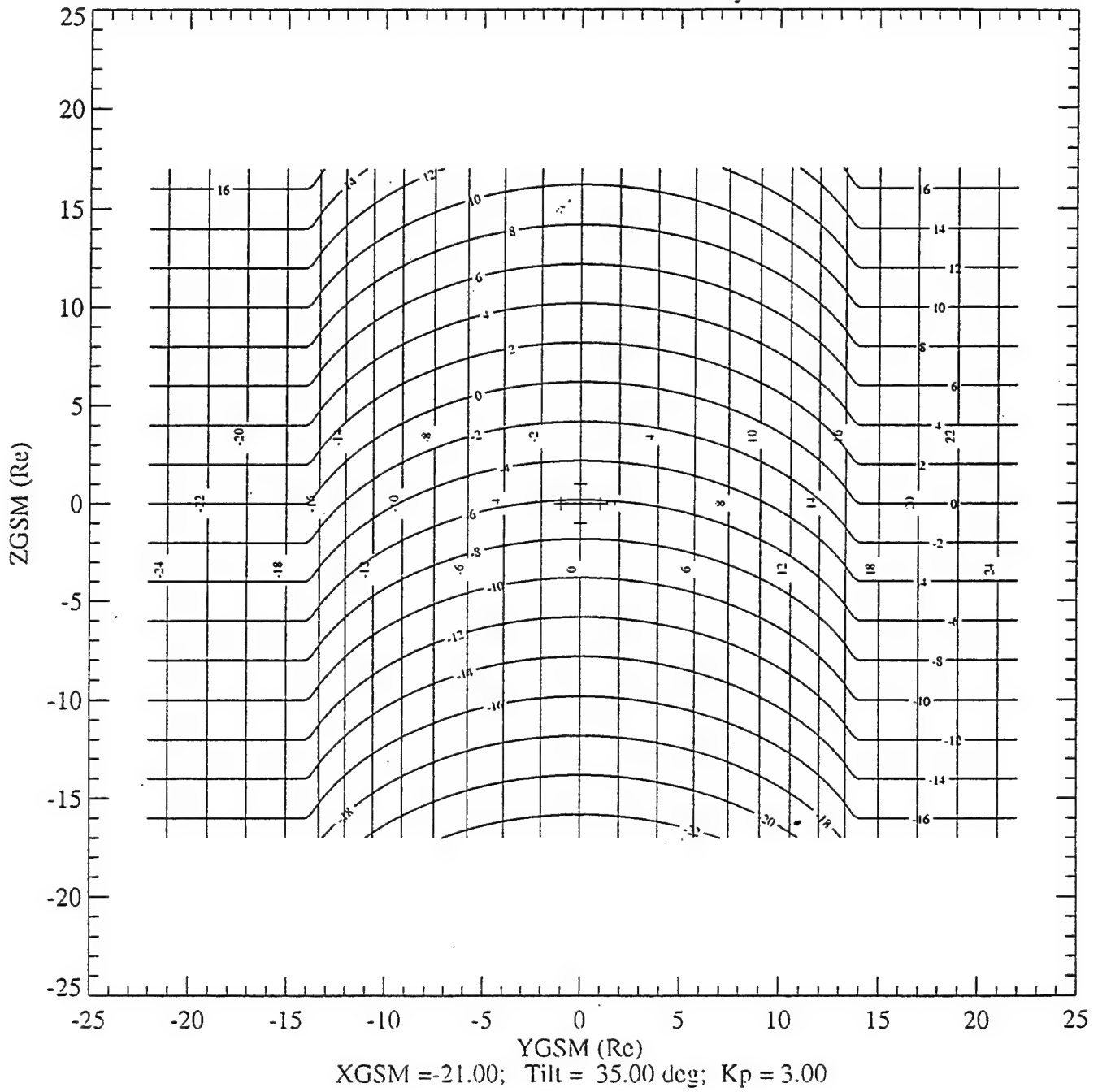
XGSM =-21.00; Tilt = 35.00 deg; Kp = 3.00

FIGURE 23

33

MSM-MAP3D Coordinate System

YGSM (Re)

XGSM =-14.00;   Tilt = 35.00 deg; Kp = 3.00

FIGURE 24

34

FIGURE 25

MSM-MAP3D Coordinate System

XGSM = 0.00;   Tilt = 35.00 deg;   Kp = 3.00
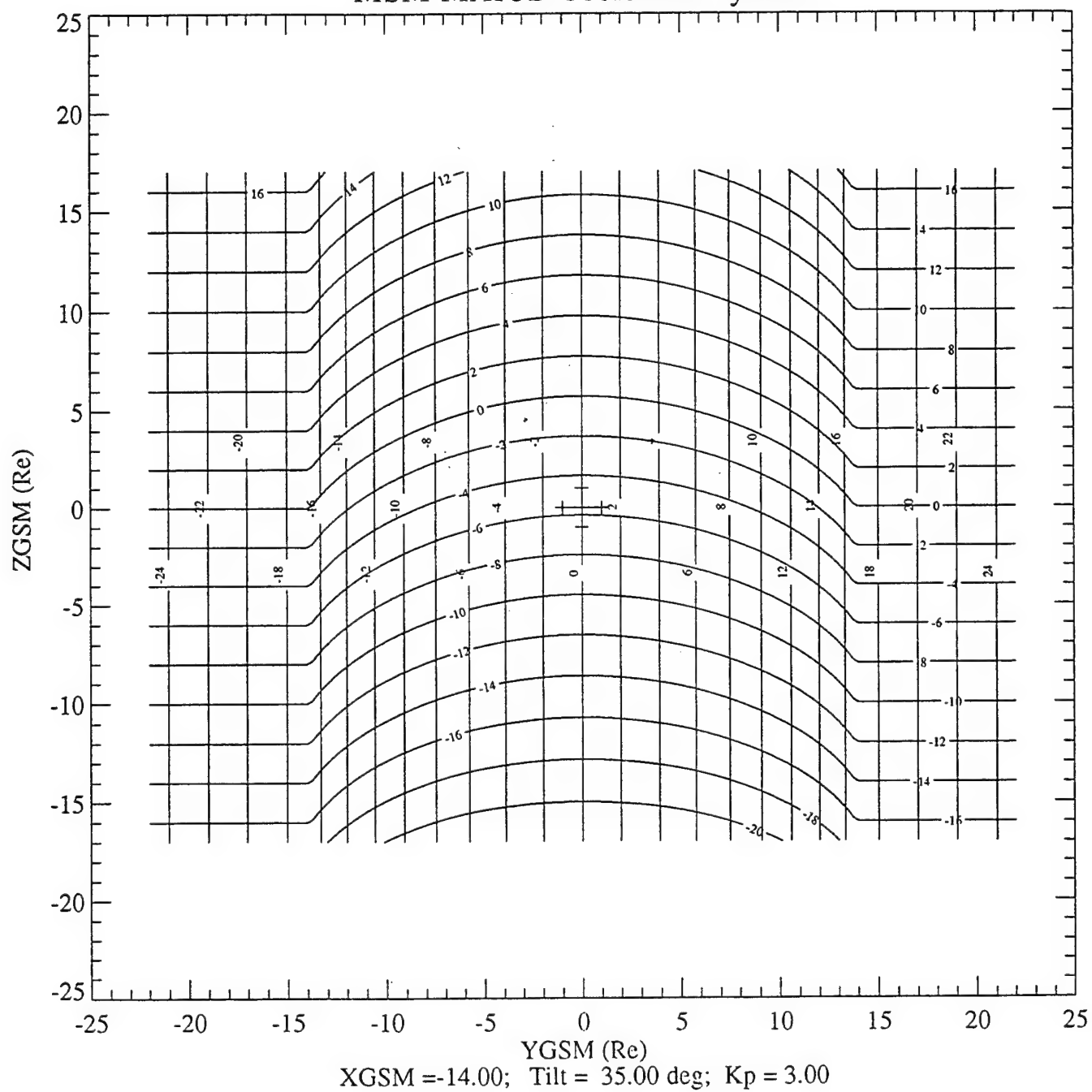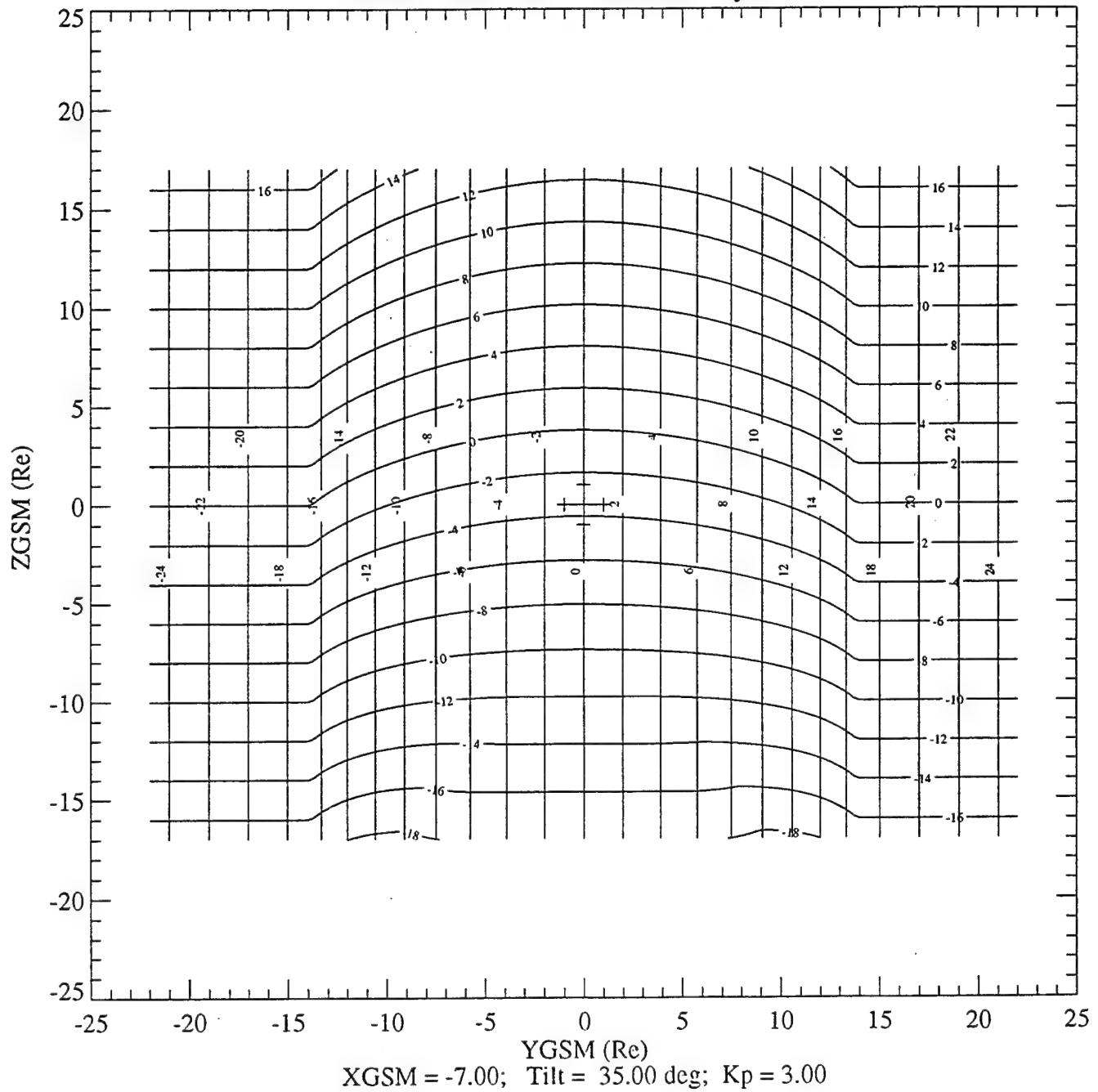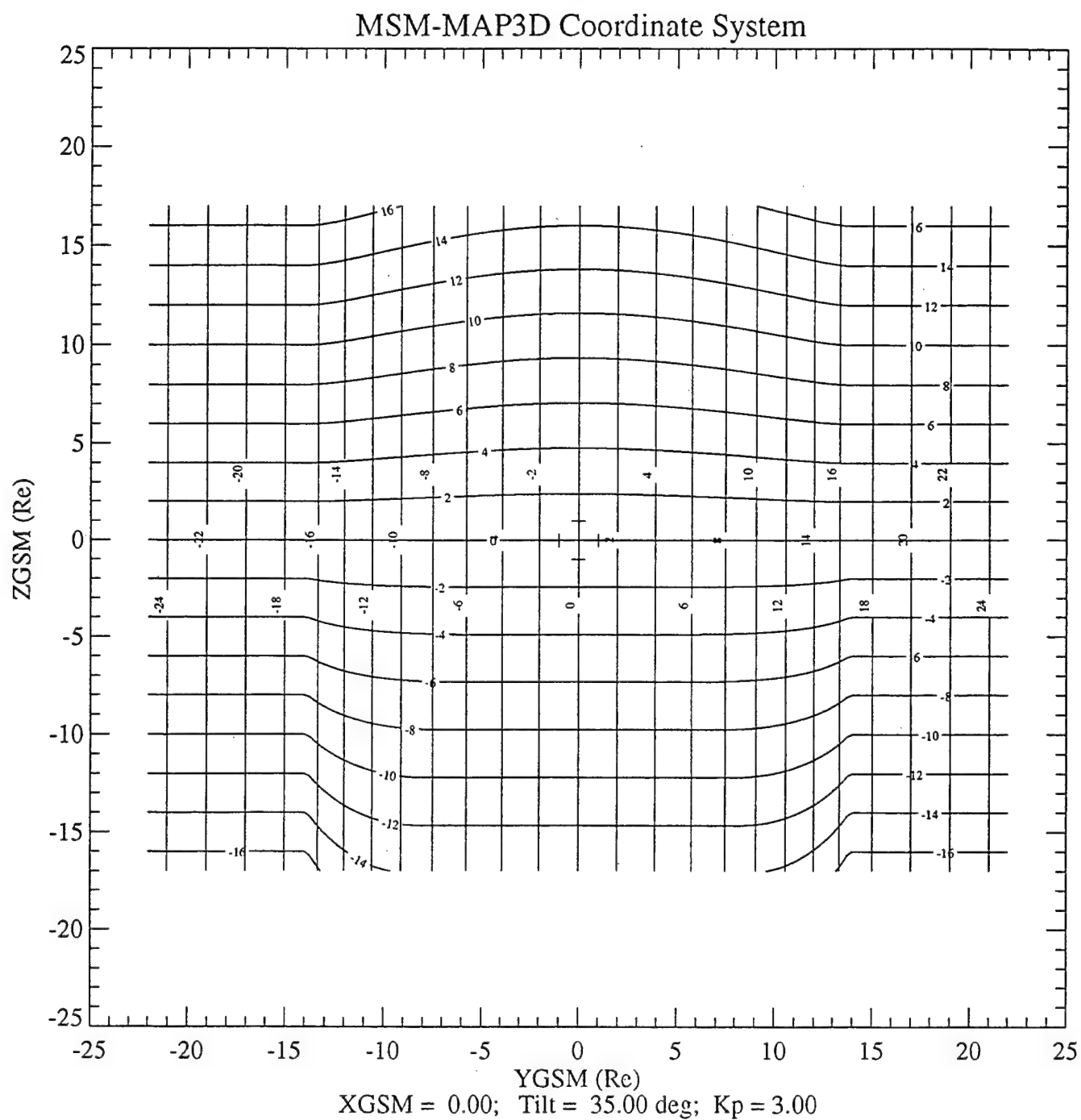
FIGURE 26

MSM-MAP3D Coordinate System

XGSM = 7.00;   Tilt = 35.00 deg; Kp = 3.00
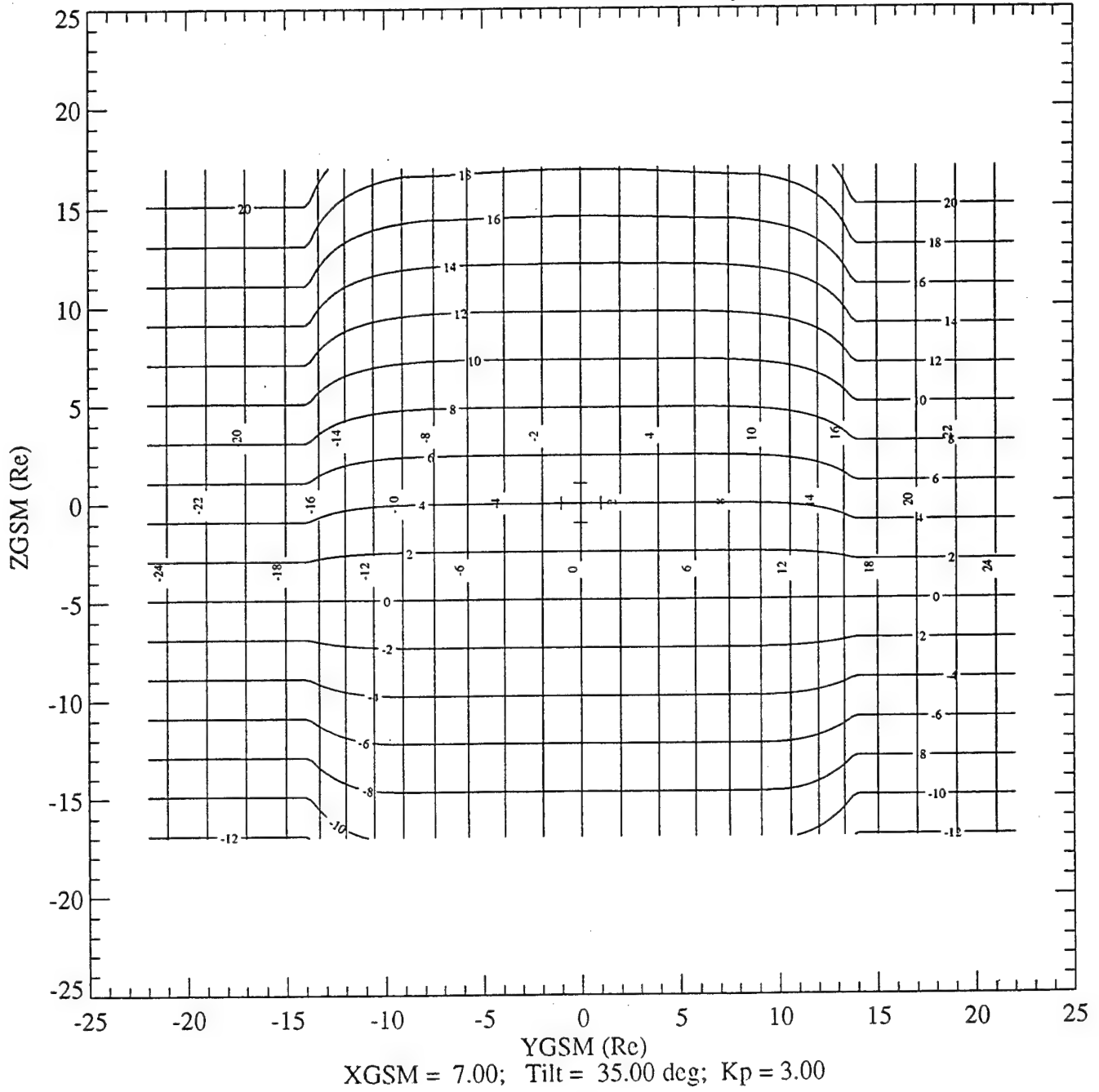
FIGURE 27

MSM-MAP3D Coordinate System

YGSM = 0.00; Tilt = 5.00 deg; Kp = 6.00
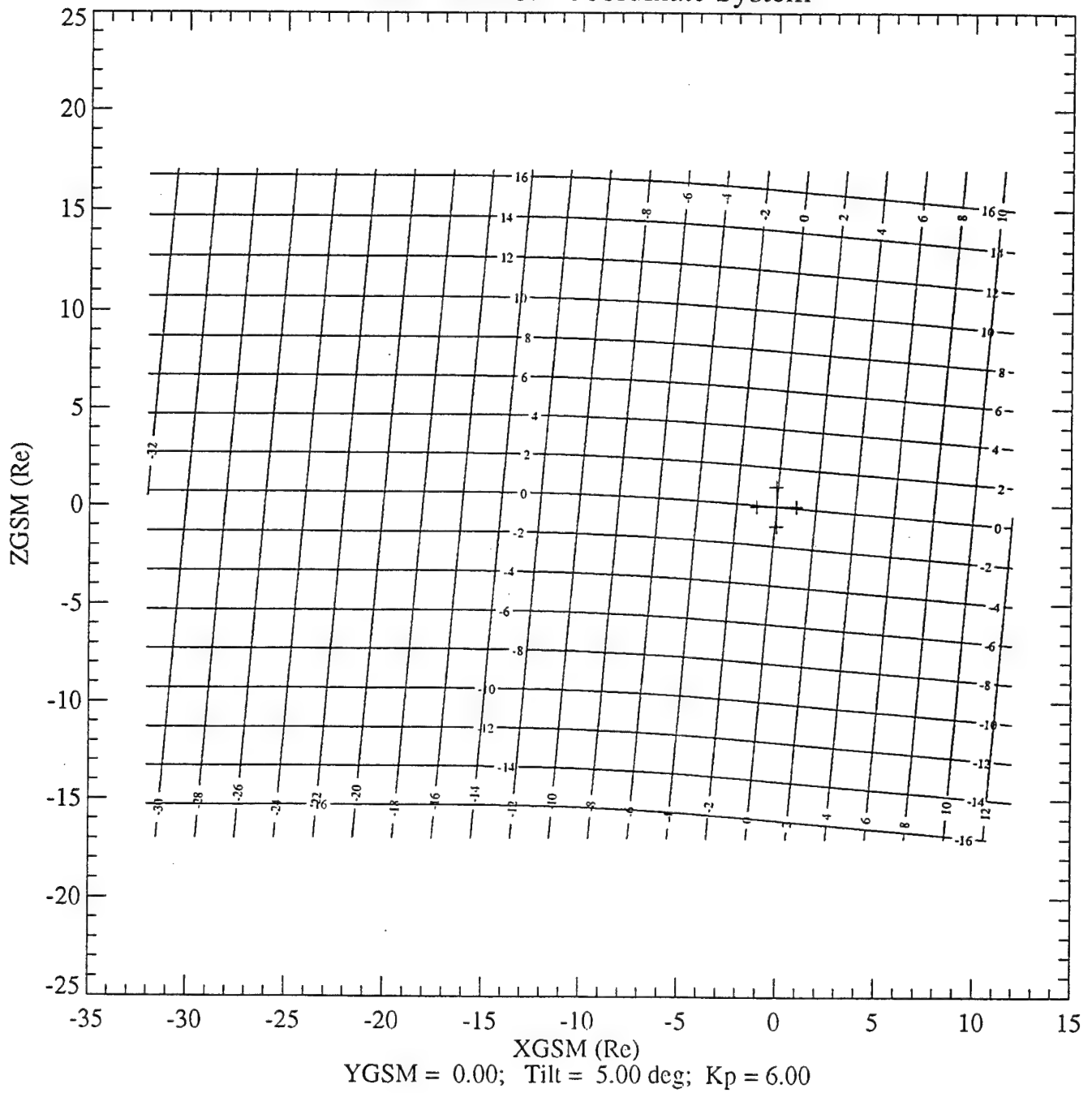
FIGURE 28

MSM-MAP3D Coordinate System

XGSM (Re)

ZGSM (Re)

YGSM = 0.00;   Tilt = 20.00 deg;   Kp = 6.00
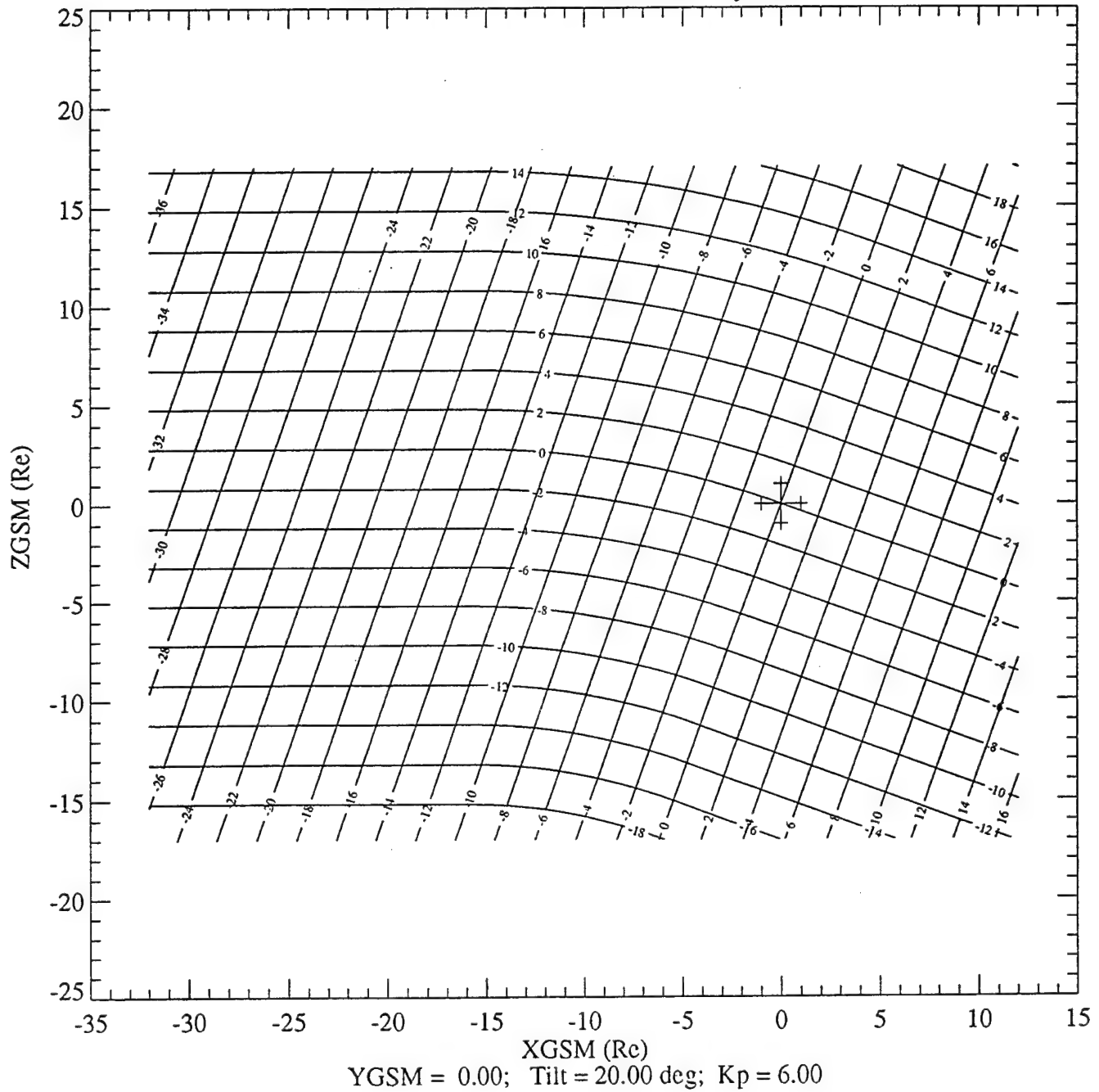
FIGURE 29

MSM-MAP3D Coordinate System

YGSM = 0.00;   Tilt = 35.00 deg;   Kp = 6.00

FIGURE 30

40

MSM-MAP3D Coordinate System

YGSM =-20.00; Tilt = 35.00 deg; Kp = 6.00

FIGURE 31

MSM-MAP3D Coordinate System

YGSM =-10.00;   Tilt = 35.00 deg; Kp = 6.00
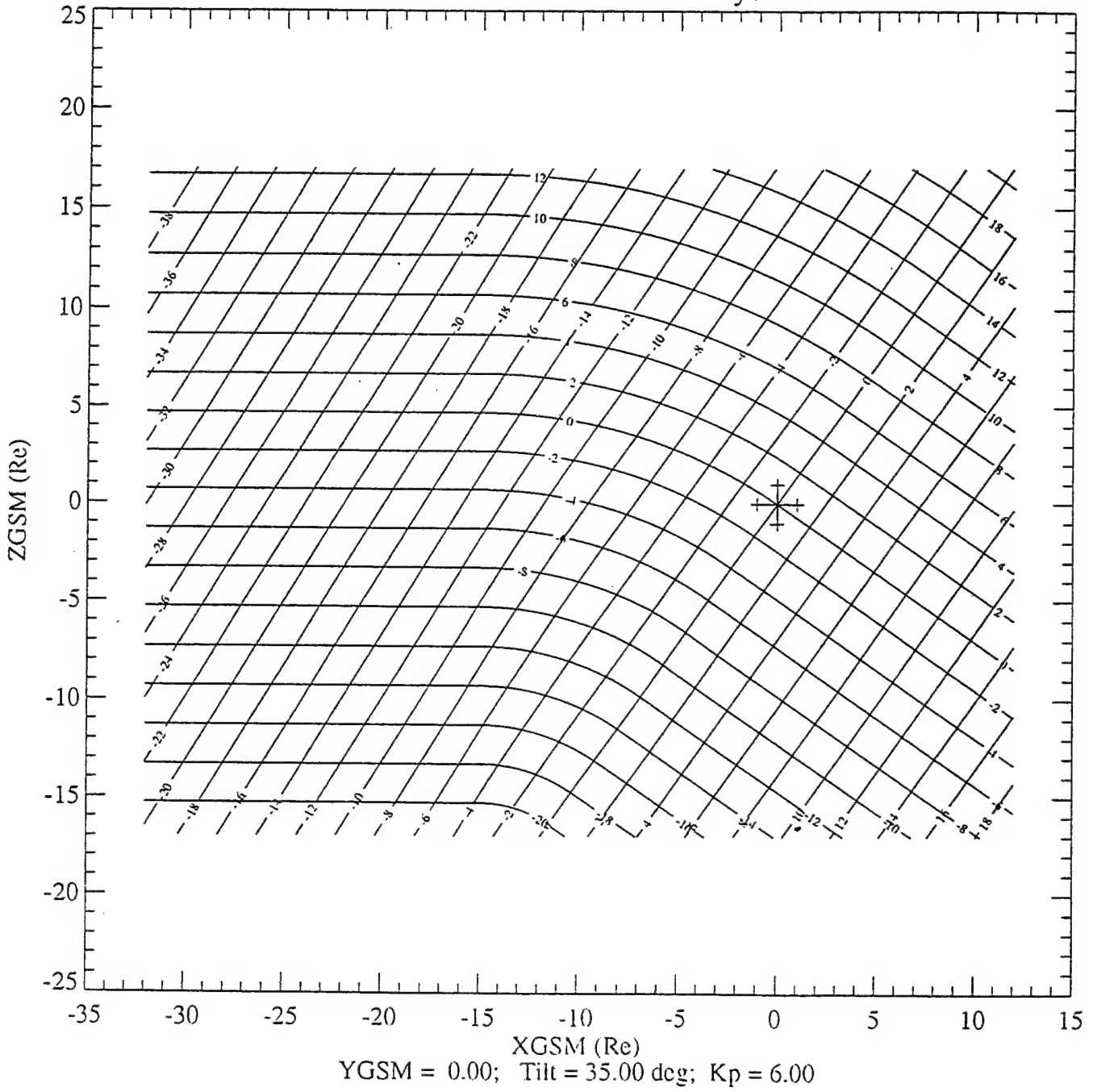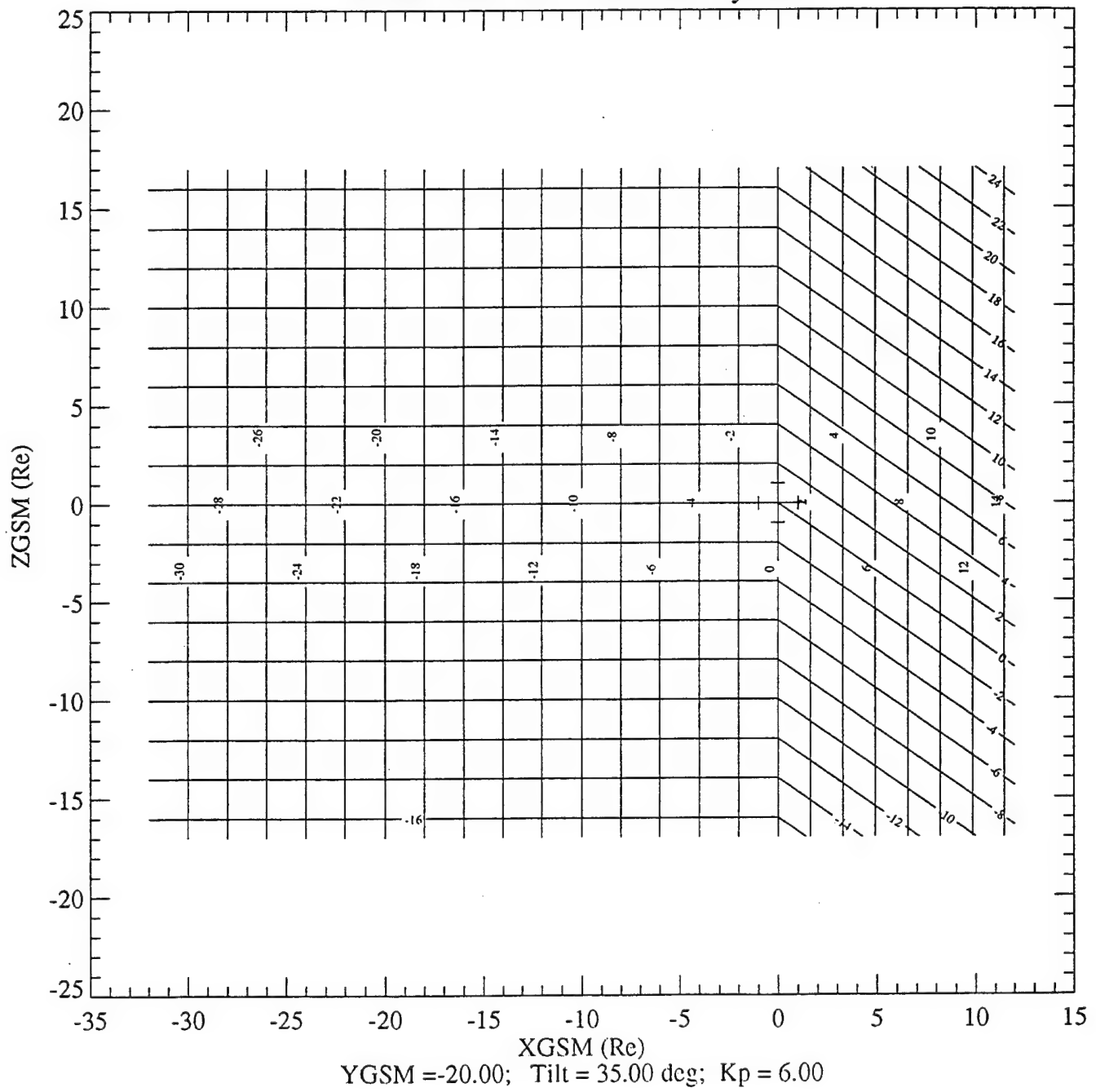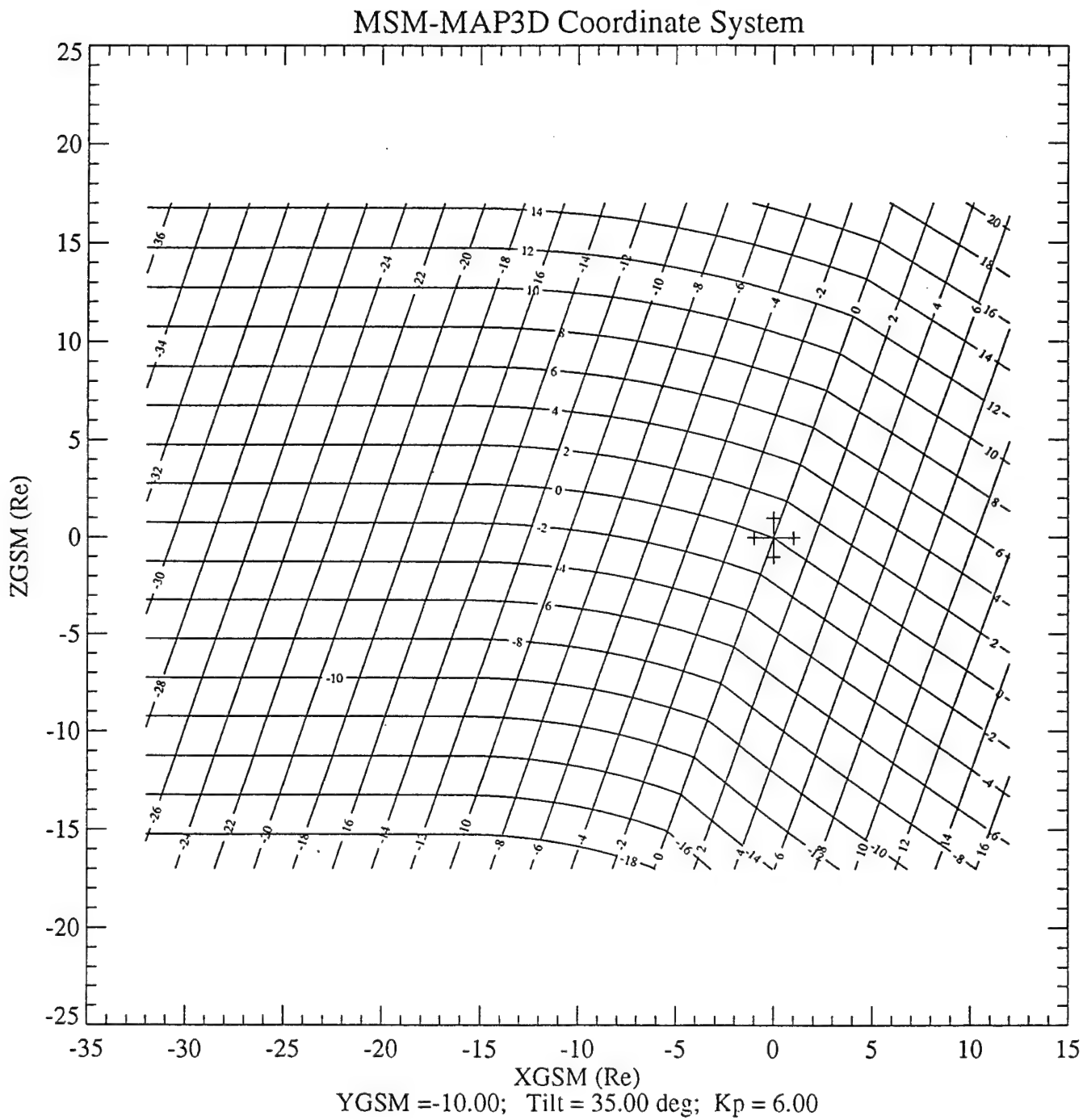
FIGURE 32

MSM-MAP3D Coordinate System

XGSM =-21.00; Tilt = 5.00 deg; Kp = 6.00

FIGURE 33

43

MSM-MAP3D Coordinate System

XGSM =-21.00; Tilt = 20.00 deg; Kp = 6.00

FIGURE 34

MSM-MAP3D Coordinate System

XGSM =-21.00;   Tilt = 35.00 deg; Kp = 6.00
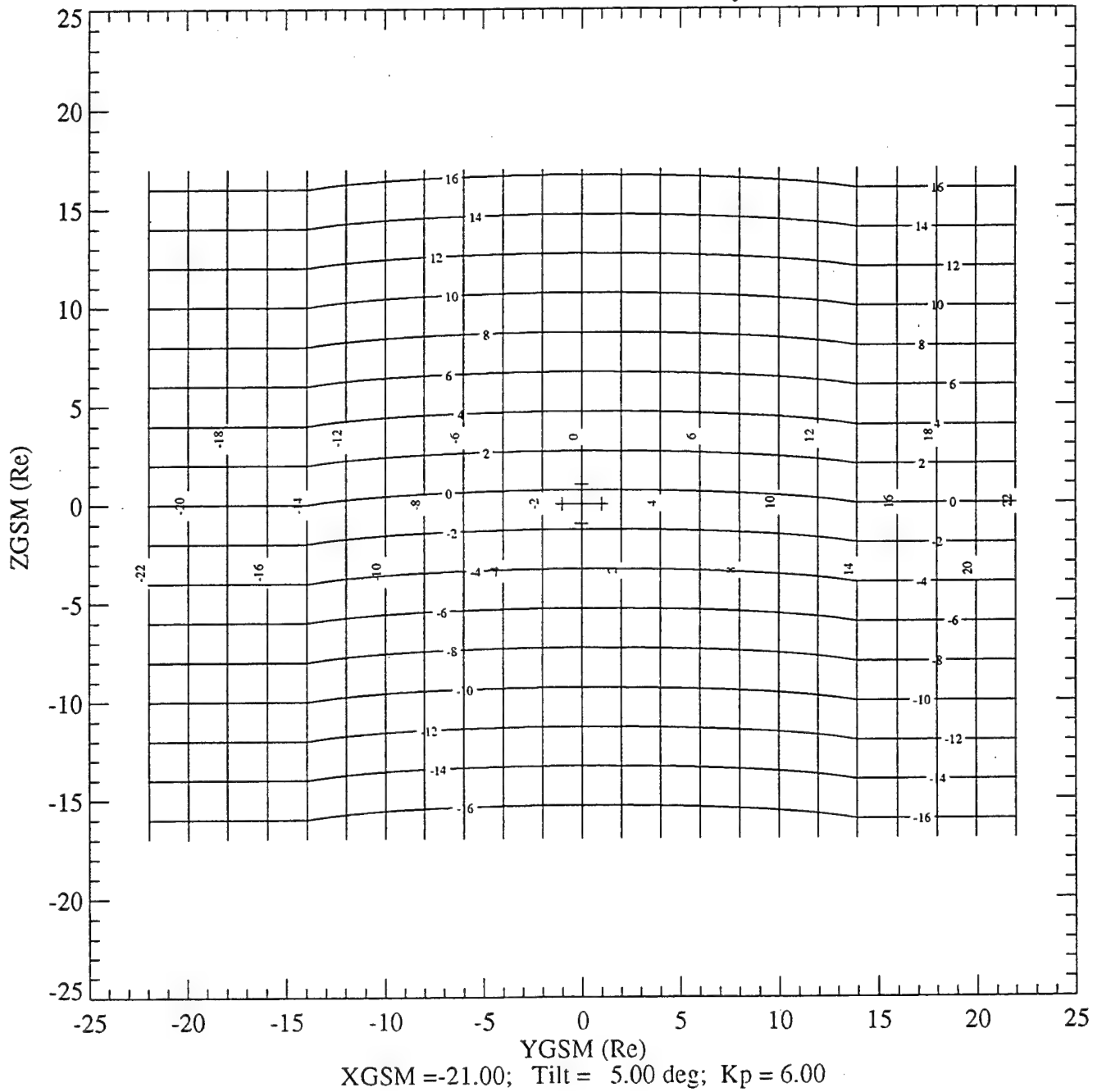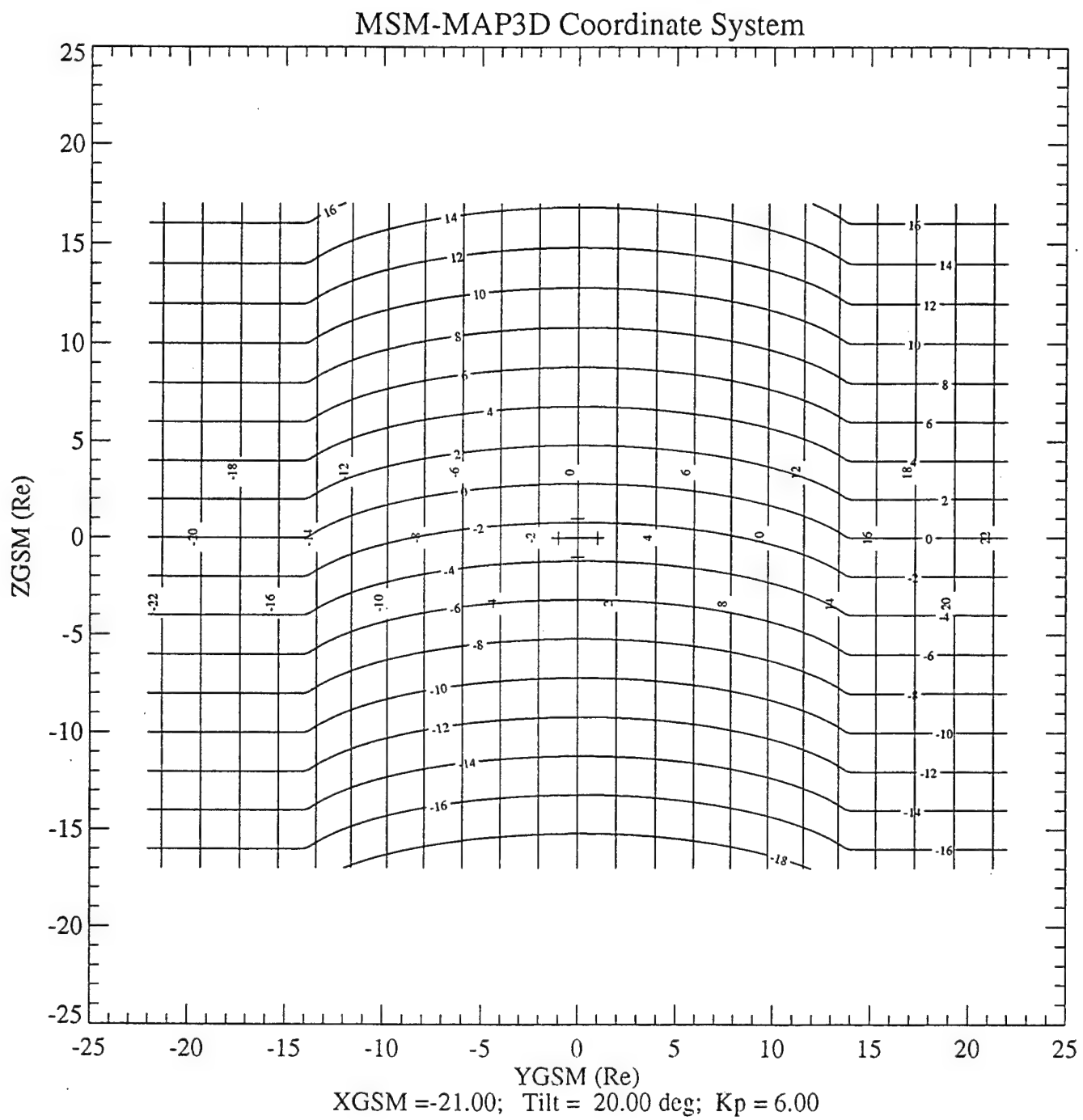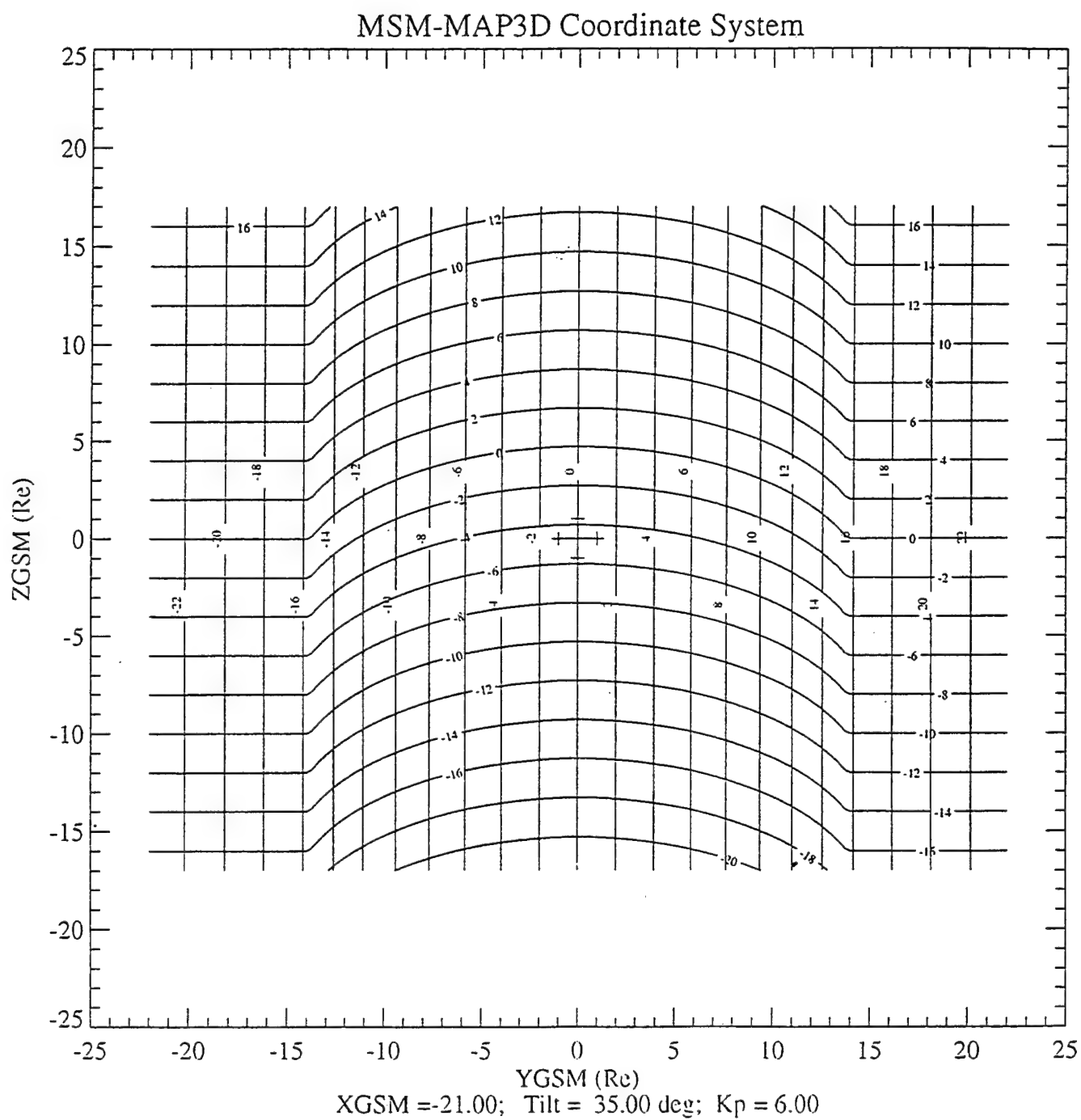
FIGURE 35

MSM-MAP3D Coordinate System

XGSM =-14.00; Tilt = 35.00 deg; Kp = 6.00
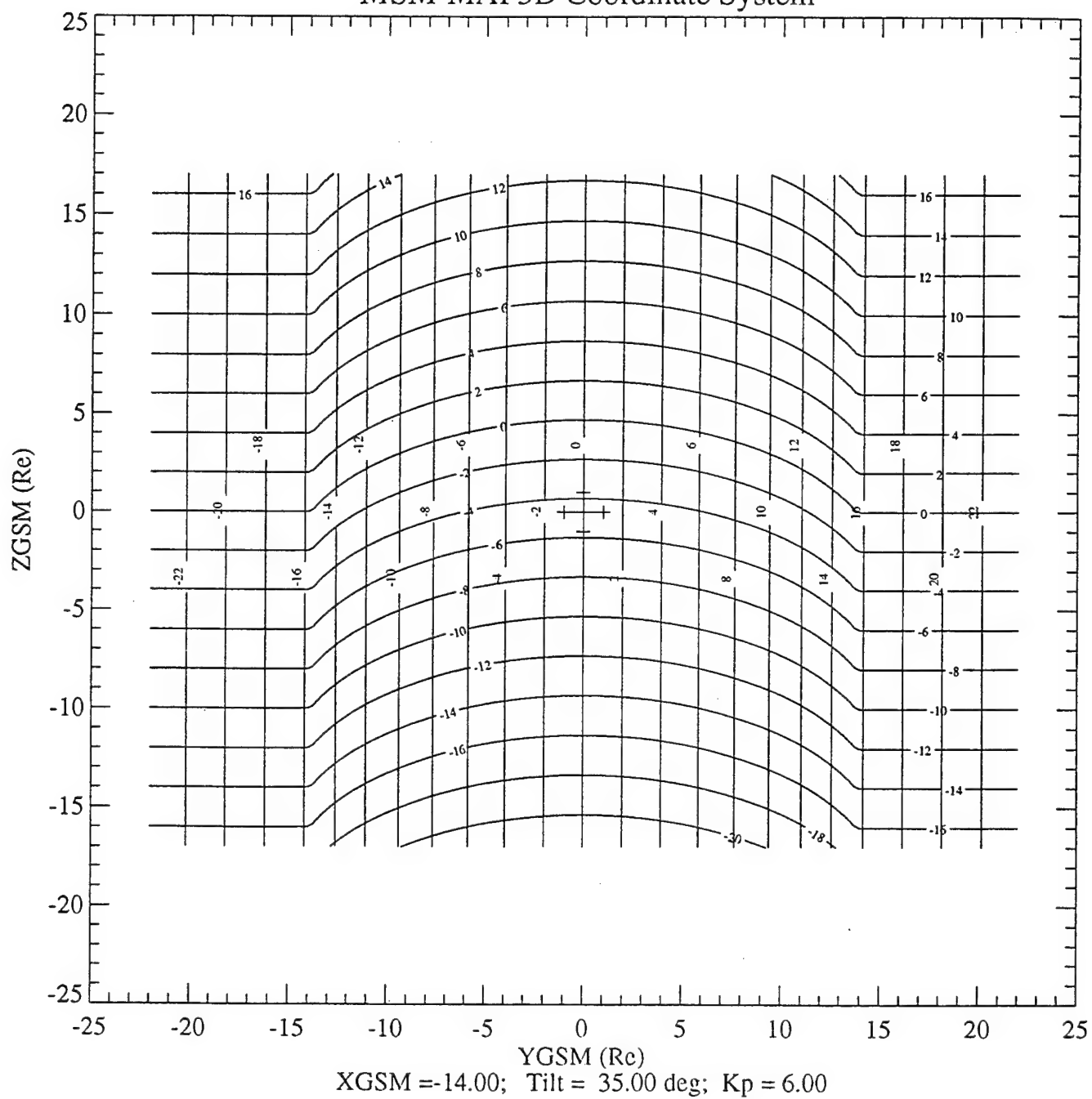
FIGURE 36

MSM-MAP3D Coordinate System

XGSM = -7.00;   Tilt = 35.00 deg; Kp = 6.00
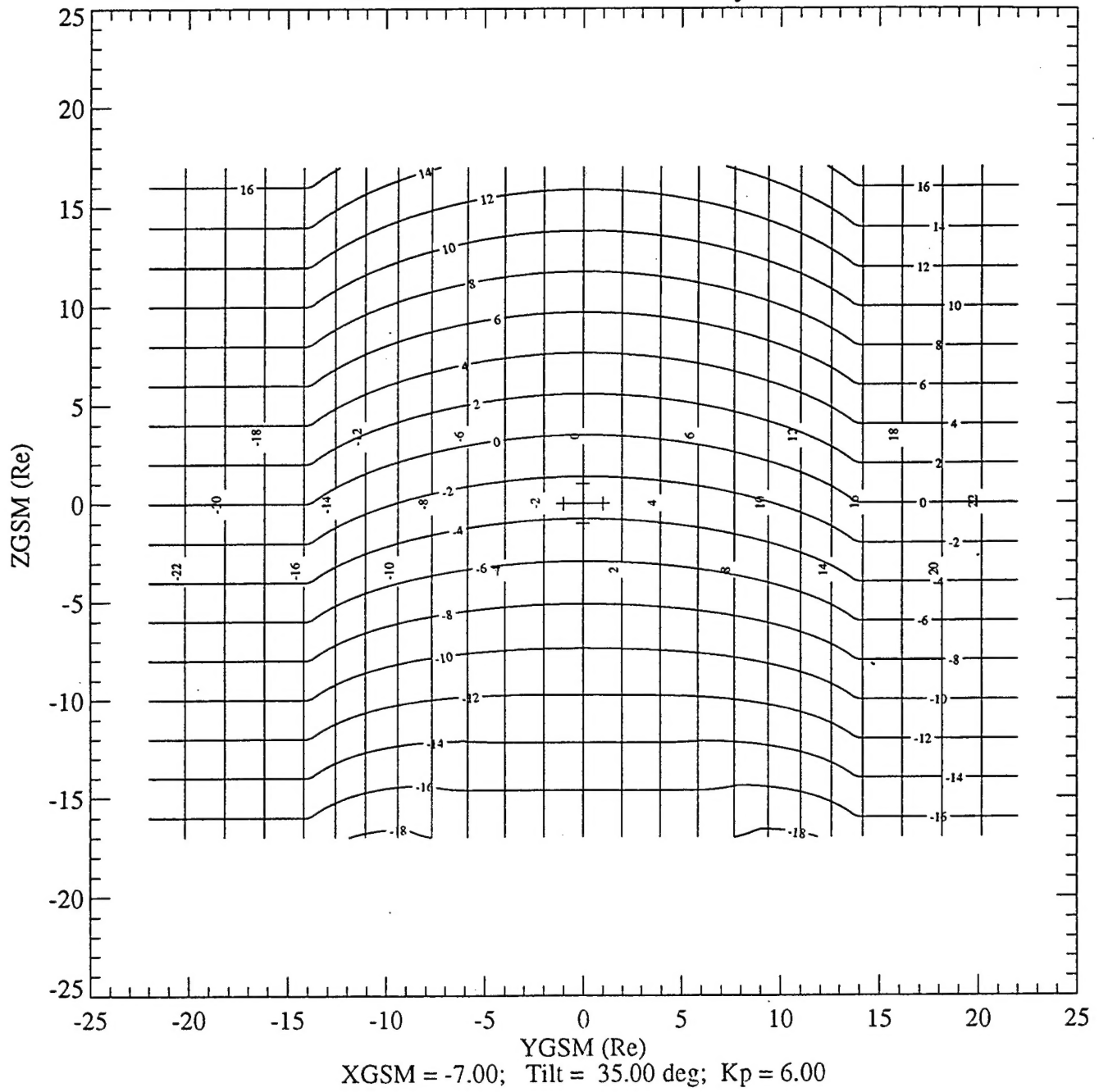
FIGURE 37

MSM-MAP3D Coordinate System

YGSM (Re)

XGSM = 0.00; Tilt = 35.00 deg; Kp = 6.00
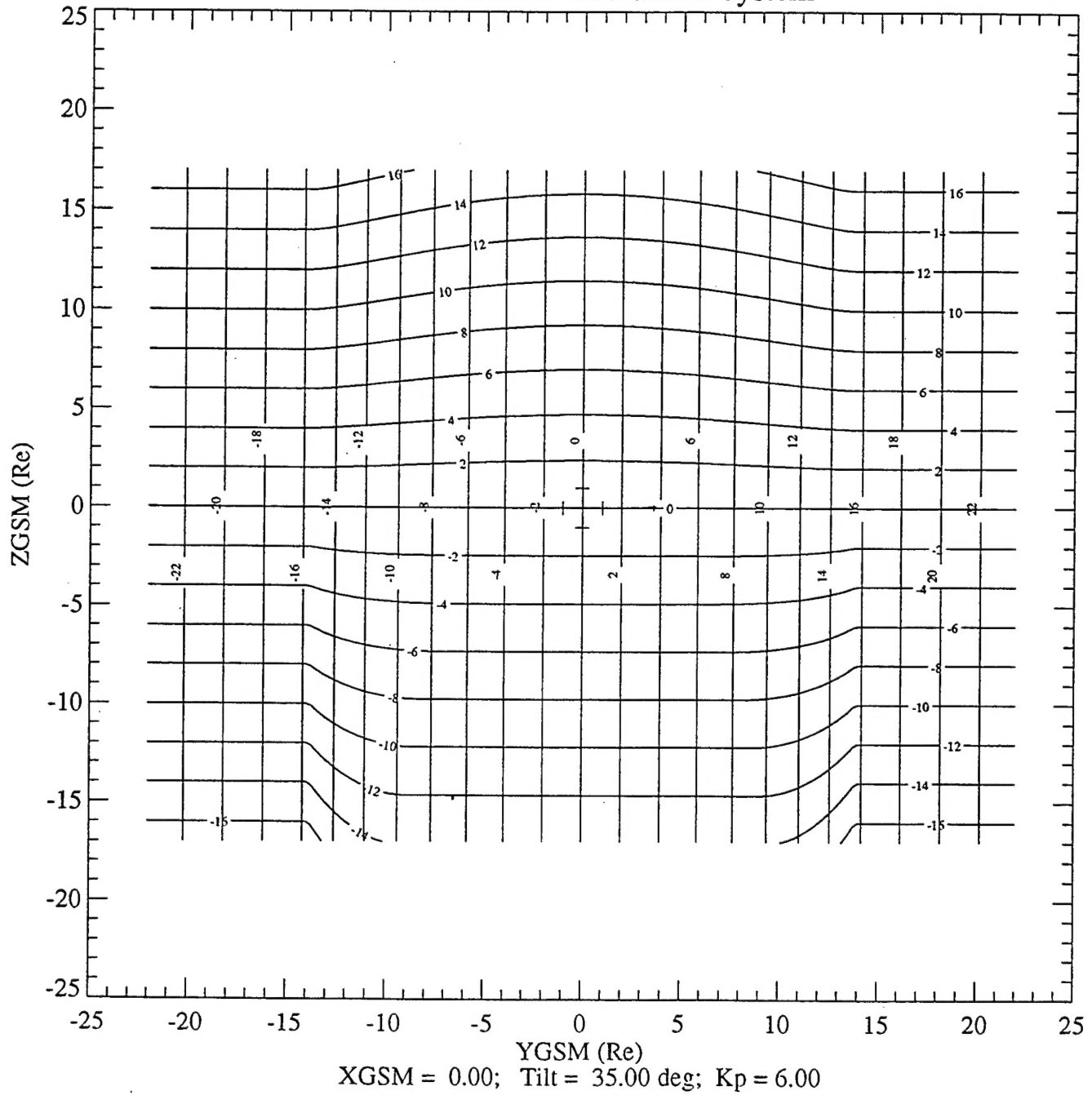
FIGURE 38

MSM-MAP3D Coordinate System

XGSM = 7.00;   Tilt = 35.00 deg; Kp = 6.00
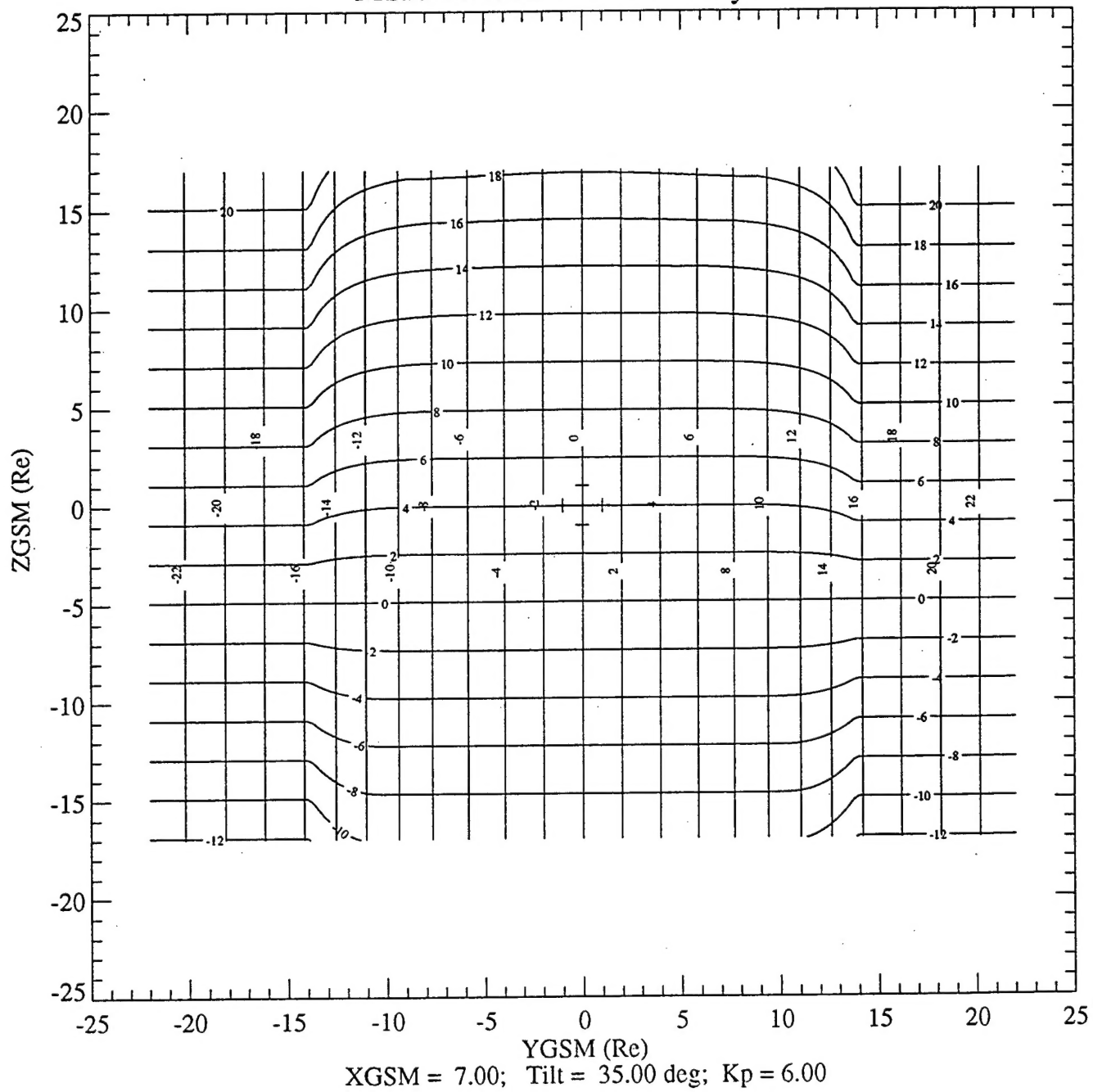
FIGURE 39

References:

Bales, B., J. Freeman, B. Hausman, R. Hilmer, R. Lambour, A. Nagai, R. Spiro, G.-H. Voigt, R. Wolf, W. F. Denig, D. Hardy, M. Heinemann, N. Maynard, F. Rich, R. D. Belian, and T. Cayton, Status of the development of the Magnetospheric Specification and Forecast Model, in *Solar-Terrestrial Predictions-IV: Proceedings of a Workshop at Ottawa, Canada, May 18-22, 1992*, ed. J. Hruska, M. A. Shea, D. F. Smart, and G. Heckman, NOAA, Environmental Res. Labs, Boulder, 467-478, 1993.

Dandouras, J., On the average shape and position of the geomagnetic neutral sheet and its influence on plasma sheet statistical studies, *J. Geophys. Res., 93*, 7345 - 7353, 1988.

Fairfield, D. H., A statistical determination of the shape and position of the geomagnetic neutral sheet, *J. Geophys. Res., 85*, 775-780, 1980.

Freeman Jr., J. W., R. A. Wolf, R. W. Spiro, G.-H. Voigt, B. A. Hausman, B. A. Bales, R. V. Hilmer, A. Nagai, and R. Lambour, Magnetospheric Specification Model: Development Code and Documentation, Rice University, 1993.

Hilmer, R. V., R. A. Wolf, and B. A. Hausman, Mapping Magnetospheric Specification Model results to arbitrary positions in the 3-D magnetosphere: Development of FORTRAN application codes MAP3D and FLUX3D, prepared for Hughes STX Corp. under subcontract No. 93-F04-I1902, Rice University, 1993.

Hilmer, R. V., and G.-H. Voigt, A magnetospheric magnetic field model with flexible current systems driven by independent physical parameters, *J. Geophys. Res., 100*, 5613-5626, 1995.

Lopez, R. E., The position of the magnetotail neutral sheet in the near-Earth region, *Geophys. Res. Lett., 17*, 1617-1620, 1990.